AD-A063 663 ARMY ENGINEER WATERWAYS EXPERIMENT STATION VICKSBURG MISS F/G 8/3
TYPE 16 FLOOD INSURANCE STUDY: TSUNAMI PREDICTIONS FOR THE WEST--ETC(U)
DEC 78 J R HOUSTON, A W GARCIA

UNCLASSIFIED WES-TR-H-78-26 NL

| OF |
AD
A063663

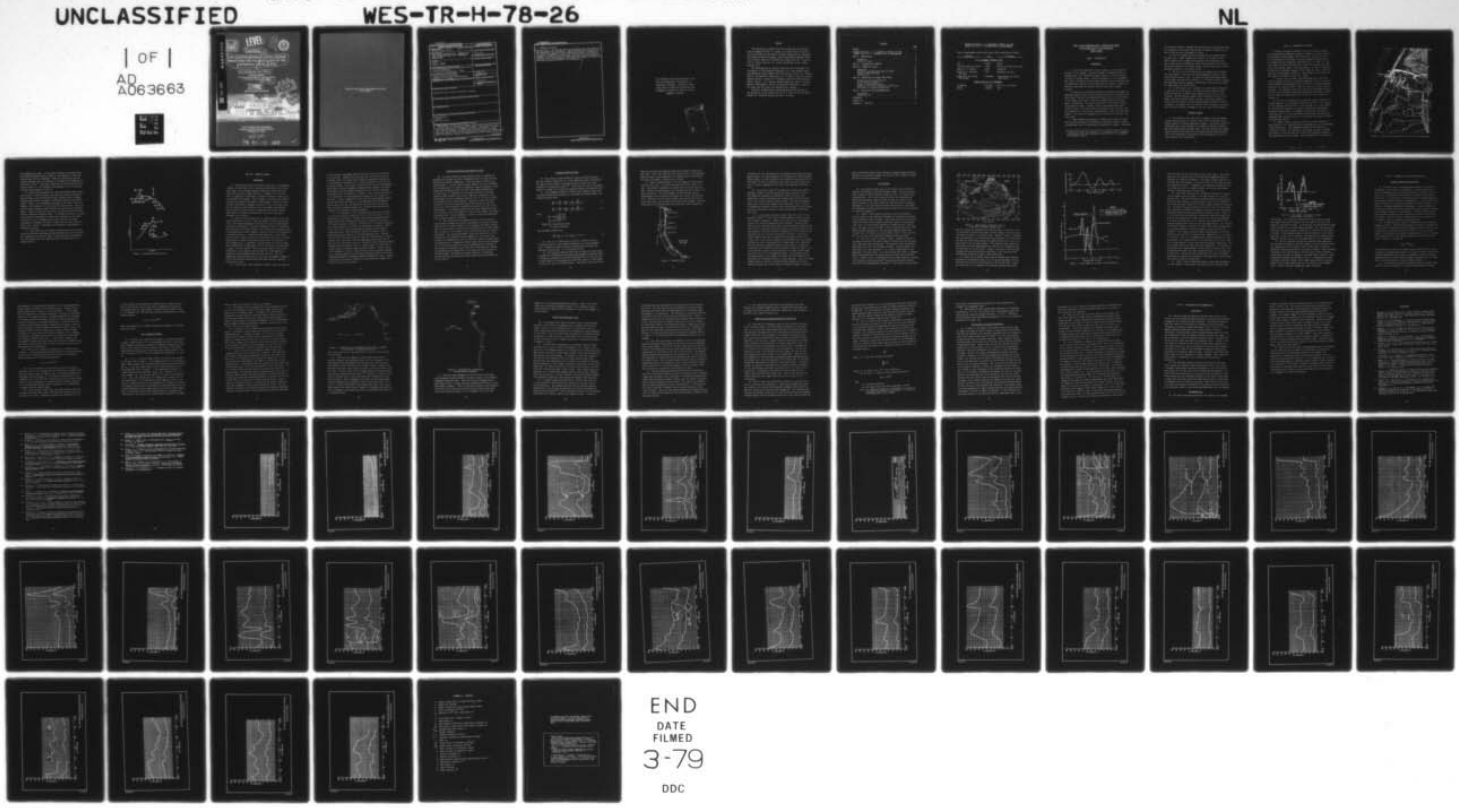

END
DATE
FILMED
3-79
DDC

LEVEL II

12

SC

(14) WES-TR-
TECHNICAL REPORT H-78-26

TYPE 16 FLOOD INSURANCE STUDY: TSUNAMI PREDICTIONS FOR THE WEST COAST OF THE CONTINENTAL UNITED STATES.

by

(10) James R. Houston Andrew W. Garcia

Hydraulics Laboratory
U. S. Army Engineer Waterways Experiment Station
P. O. Box 631, Vicksburg, Miss. 39180

(12) 73 P.

(11) Dec 78

(9) Final Report.

Prepared for Federal Insurance Administration
Department of Housing and Urban Development
Washington, D. C. 20314

Destroy this report when no longer needed. Do not return it to the originator.

Unclassified

SECURITY CLASSIFICATION OF THIS PAGE (When Data Entered)

REPORT DOCUMENTATION PAGE		READ INSTRUCTIONS BEFORE COMPLETING FORM
1. REPORT NUMBER Technical Report H-78-26	2. GOVT ACCESSION NO.	3. RECIPIENT'S CATALOG NUMBER
4. TITLE (and Subtitle) TYPE 16 FLOOD INSURANCE STUDY: TSUNAMI PREDICTIONS FOR THE WEST COAST OF THE CONTINENTAL UNITED STATES		5. TYPE OF REPORT & PERIOD COVERED Final report 6. PERFORMING ORG. REPORT NUMBER
7. AUTHOR(s) James R. Houston Andrew W. Garcia		8. CONTRACT OR GRANT NUMBER(s)
9. PERFORMING ORGANIZATION NAME AND ADDRESS U. S. Army Engineer Waterways Experiment Station Hydraulics Laboratory P. O. Box 631, Vicksburg, Miss. 39180		10. PROGRAM ELEMENT, PROJECT, TASK AREA & WORK UNIT NUMBERS
11. CONTROLLING OFFICE NAME AND ADDRESS Federal Insurance Administration Department of Housing and Urban Development Washington, D. C. 20314		12. REPORT DATE December 1978 13. NUMBER OF PAGES 69
14. MONITORING AGENCY NAME & ADDRESS(if different from Controlling Office)		15. SECURITY CLASS. (of this report) Unclassified 15a. DECLASSIFICATION/DOWNGRADING SCHEDULE

16. DISTRIBUTION STATEMENT (of this Report)

Approved for public release; distribution unlimited.

17. DISTRIBUTION STATEMENT (of the abstract entered in Block 20, if different from Report)

18. SUPPLEMENTARY NOTES

19. KEY WORDS (Continue on reverse side if necessary and identify by block number)

Flood insurance
Tsunamis
Water wave run-up

20. ABSTRACT (Continue on reverse side if necessary and identify by block number)

Calculations of runup due to tsunamis of distant origin were made for most of the west coast of the continental United States. Runup values were determined that were expected to be equaled or exceeded on the average of once per 100 or once per 500 years. Historical data of tsunami activity in distant generation regions were used in the investigation in conjunction with numerical models that generated tsunamis and propagated them across the deep-ocean and

(Continued)

DD FORM 1 JAN 73 1473 EDITION OF 1 NOV 65 IS OBSOLETE

Unclassified

SECURITY CLASSIFICATION OF THIS PAGE (When Data Entered)

20. ABSTRACT (Continued).

nearshore region. The combined effects of astronomical tides and tsunamis were also incorporated into the analysis. Numerical simulations of actual historical tsunamis and comparisons of calculations with tide gage recordings were presented. Calculations of tsunami runup based upon data of local historical tsunamis (at the few locations on the west coast where there were sufficient historical data to allow reasonable predictions) were compared with predictions based upon the methods presented in the investigation.

THE CONTENTS OF THIS REPORT ARE NOT TO BE USED FOR ADVERTISING, PUBLICATION, OR PROMOTIONAL PURPOSES. CITATION OF TRADE NAMES DOES NOT CONSTITUTE AN OFFICIAL ENDORSEMENT OR APPROVAL OF THE USE OF SUCH COMMERCIAL PRODUCTS.

PREFACE

The investigation reported herein was authorized by the Office, Chief of Engineers (OCE), U. S. Army, in a letter dated 24 June 1975 and was performed for the Federal Insurance Administration, Department of Housing and Urban Development, under Inter-Agency Agreements IAA-H-16-75, Project Order No. 23; IAA-H-7-76, Project Order No. 2; and IAA H-10-77, Project Order No. 30. Project coordinator was Mr. Jerome Peterson, OCE.

The investigation was conducted from July 1975 to November 1977 by personnel of the Hydraulics Laboratory, U. S. Army Engineer Waterways Experiment Station (WES), under the direction of Mr. H. B. Simmons, Chief of the Hydraulics Laboratory, Dr. R. W. Whalin, Chief of the Wave Dynamics Division, and Mr. D. D. Davidson, Chief of the Wave Research Branch. Messrs. J. R. Houston, Research Physicist, and A. W. Garcia, Research Oceanographer, both of the Hydraulics Laboratory, conducted the study; and this report was prepared by Mr. Houston.

Directors of WES during the investigation and the preparation and publication of this report were COL G. H. Hilt, CE, and COL John L. Cannon, CE. Technical Director was Mr. F. R. Brown.

CONTENTS

CONVERSION FACTORS, U. S. CUSTOMARY TO METRIC (SI) AND METRIC (SI) TO U. S. CUSTOMARY UNITS OF MEASUREMENTS

Units of measurement used in this report can be converted as follows:

Multiply	By	To Obtain
U. S. Customary to Metric (SI)		
feet	0.3048	metres
feet per second per second	0.3048	metres per second per second
miles (U. S. statute)	1.852	kilometres
miles (U. S. nautical) per hour	1.852	kilometres per hour
square feet per second per second	0.09290304	square metres per second per second
Metres (SI) to U. S. Customary		
kilometres	0.6213711	miles (U. S. statute)
metres	3.280839	feet

TYPE 16 FLOOD INSURANCE STUDY: TSUNAMI PREDICTIONS FOR THE WEST COAST OF THE CONTINENTAL UNITED STATES

PART I: INTRODUCTION

Background

1. Of all water waves that occur in nature, one of the most destructive is the tsunami. The term "tsunami," originating from the Japanese words "tsu" (harbor) and "nami" (wave), is used to describe sea waves of seismic origin. Tectonic earthquakes, i.e., earthquakes that cause a deformation of the seabed, appear to be the principal seismic mechanism responsible for the generation of tsunamis. Coastal and submarine landslides and volcanic eruptions also have triggered tsunamis.

2. Tsunamis are principally generated by undersea earthquakes of magnitudes greater than 6.5 on the Richter scale with focal depths less than 50 km.* They are very long-period waves (5 min to several hours) of low height (a few feet or less) when traversing water of oceanic depth. Consequently, they are not discernible in the deep ocean and go unnoticed by ships. Tsunamis travel at the shallow-water wave celerity equal to the square root of acceleration due to gravity times water depth even in the deepest oceans because of their very long wavelengths. This speed of propagation can be in excess of 500 mph in the deep ocean.

3. When tsunami waves approach a coastal region where the water depth decreases rapidly, wave refraction, shoaling, and bay or harbor resonance may result in significantly increased wave heights. The great

---

* A table of factors for converting U. S. customary units of measurement to metric (SI) units and metric (SI) units to U. S. customary is presented on page 4.

period and wavelength of tsunami waves preclude their dissipating energy as a breaking surf; instead, they are apt to appear as rapidly rising water levels and only occasionally as bores.

4. Over 500 tsunamis have been reported within recorded history. Virtually all of these tsunamis have occurred in the Pacific Basin. This is because most tsunamis are associated with earthquakes, and most seismic activity beneath the oceans is concentrated in the narrow fault zones adjacent to the great oceanic trench systems which are predominantly confined to the Pacific Ocean.

5. The loss of life and destruction of property due to tsunamis have been immense. The Great Hoei Tokaido-Nankaido tsunami of Japan killed 30,000 people in 1707. In 1868, the Great Peru tsunami caused 25,000 deaths and carried the frigate U. S. S. Waterlee 1,300 ft inland. The Great Meiji Sanriku tsunami of 1896 killed 27,122 persons in Japan and washed away over 10,000 houses.

6. In recent times, three tsunamis have caused major destruction in areas of the United States. The Great Aleutian tsunami of 1946 killed 173 persons in Hawaii, where heights as great as 55 ft were recorded. The 1960 Chilean tsunami killed 330 people in Chile, 61 in Hawaii, and 199 in distant Japan. The most recent major tsunami to affect the United States, the 1964 Alaskan tsunami, killed 107 people in Alaska, 4 in Oregan, and 11 in Crescent City, California, and caused over 100 million dollars in damage on the west coast of North America.

Purpose of Study

7. The purpose of this study was to establish 100- and 500-year tsunami runup elevations on the west coast of the continental United States produced by distantly generated tsunamis. Two earlier reports[1,2] established these runup elevations for Southern California, Monterey Bay, San Francisco Bay, and Puget Sound. The 100- and 500-year tsunami runup elevations are required by the Federal Insurance Administration (FIA) of the Department of Housing and Urban Development for use in flood insurance rate calculations.

PART II: EXPLANATION OF RESULTS

8. Plates 1-30 present predicted 100- and 500-year elevations (in feet) produced by distantly generated tsunamis on the west coast of the continental United States. These elevations include the effects of the astronomical tide; that is, they are maximum elevations due to the superposition of tsunami and tidal wave forms (see PART IV). The lower curves in Plates 1-30 represent the 100-year runup and the upper curves, the 500-year runup. A 100-year runup is one that is equaled or exceeded with an average frequency of once every 100 years; a 500-year runup has a corresponding definition. Runup values in this report are referenced to the mean sea level (msl) datum.

9. Plates 1 and 2 present 100- and 500-year runup elevations versus longitude in minutes. These two plates only cover a section of coast extending from longitude 119°45' to 120°30', (from Santa Barbara, California, to latitude 34°30'). This is a section of coast oriented east-west. The remainder of the west coast has a north-south orientation and 100- and 500-year runup elevations versus latitudes in minutes for this coast (extending from 34°30' to 48°23.6') are presented in Plates 3-30.

10. In order to determine 100- or 500-year runup elevations at a coastal location, it is necessary to know the latitude of the location (or the longitude of the location if the latitude is less than 34°30'). The latitude and longitude of a coastal location can be determined using most standard maps. For example, the National Ocean Survey (previously the U. S. Coast and Geodetic Survey) maps and topographic quadrangle maps published by the U. S. Geological Survey have latitude and longitude markings.

11. Figure 1 shows a section of coast in northern California taken from the U. S. Geological Survey quadrangle map entitled "Cannibal Island, California." This quadrangle extends from a latitude of 40°37'30" to 40°45'. The section of coast shown in Figure 1 extends from 40°40' to 40°42'30" with the 40' and 42'30" markings located on the right-hand side of the figure. The 40° marking is on a section of

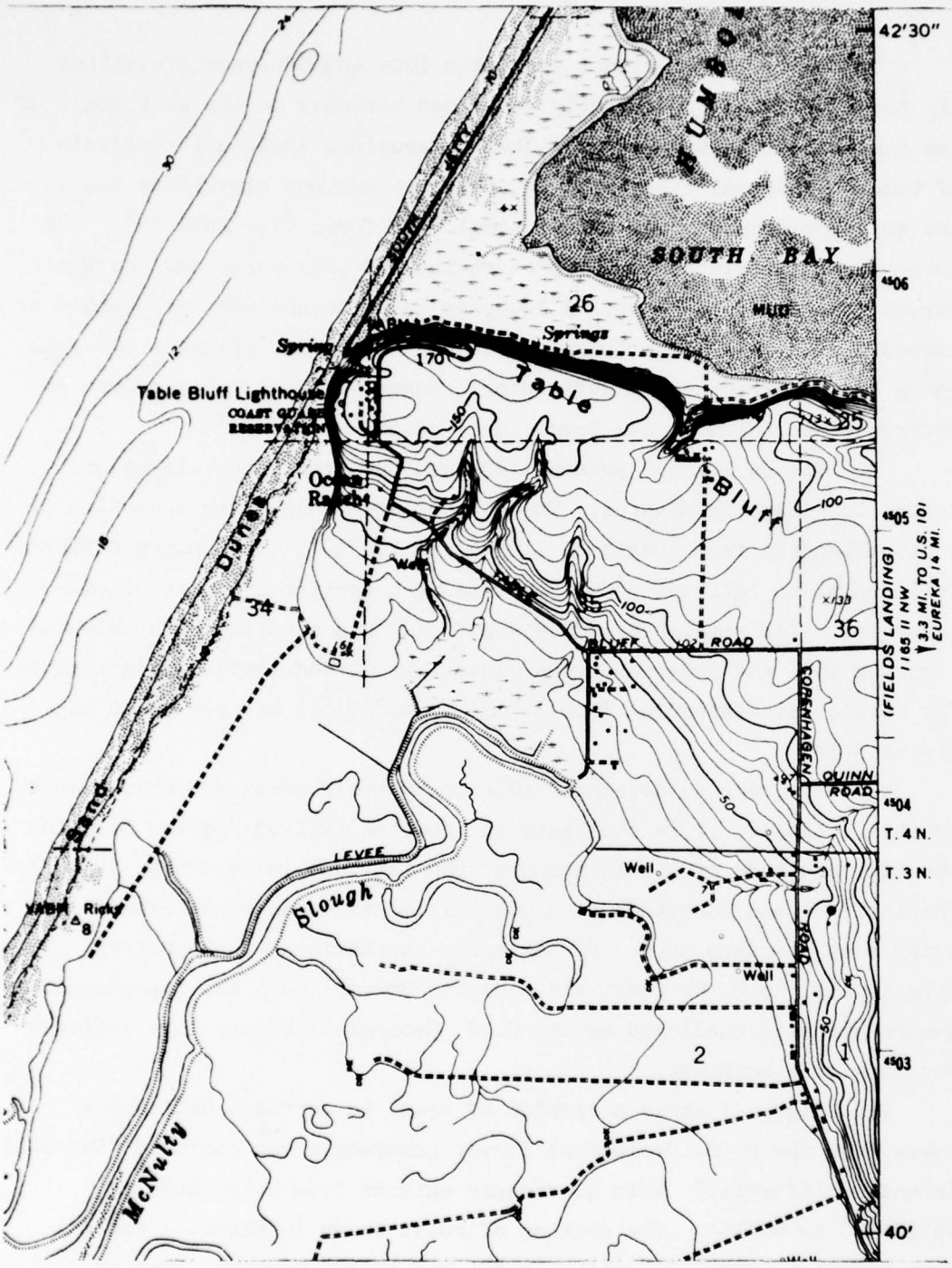

Figure 1. Section of Cannibal Island, California, quadrangle map

the quadrangle not shown. If the runup elevations are needed at the Table Bluff Lighthouse shown in Figure 1, the latitude of this coast location must first be determined. Using an ordinary ruler and the latitude markings given, the latitude of the Table Bluff Lighthouse is found to be 40°41.7". The runup elevations for this latitude are presented in Plate 15. The 100-year runup elevation is 10.2 ft and the 500-year runup elevation is 20.6 ft.

12. Several bays along the west coast have multiple-valued coastlines (that is, within and near a bay there are locations having the same latitude); these are San Luis Obispo, Bolinas, Drake's, Bodega, Trinidad, and Crescent City Bays in California and Port Orford Bay in Oregon. Figure 2 is an illustrative drawing of such bays. Note, for example, that locations 4, 6, and 9 have the same latitude. Thus, the plots of runup elevation versus latitude must necessarily be multiple-valued. Figure 2 shows that locations 4, 6, and 9 have the same latitude but different elevation values. To eliminate confusion as to which runup elevation corresponds to a particular latitude, the following convention is used: movement along a coast from south to north corresponds to movement from left to right along the runup curves in Plates 3-30. Figure 2 illustrates this convention using numbers to represent locations.

13. This report does not present runup elevations for the California coast between San Diego and Santa Barbara since such elevations were presented in an earlier report.[1] Runup elevations for Monterey Bay, San Francisco Bay, and Puget Sound were also presented in an earlier report.[2]

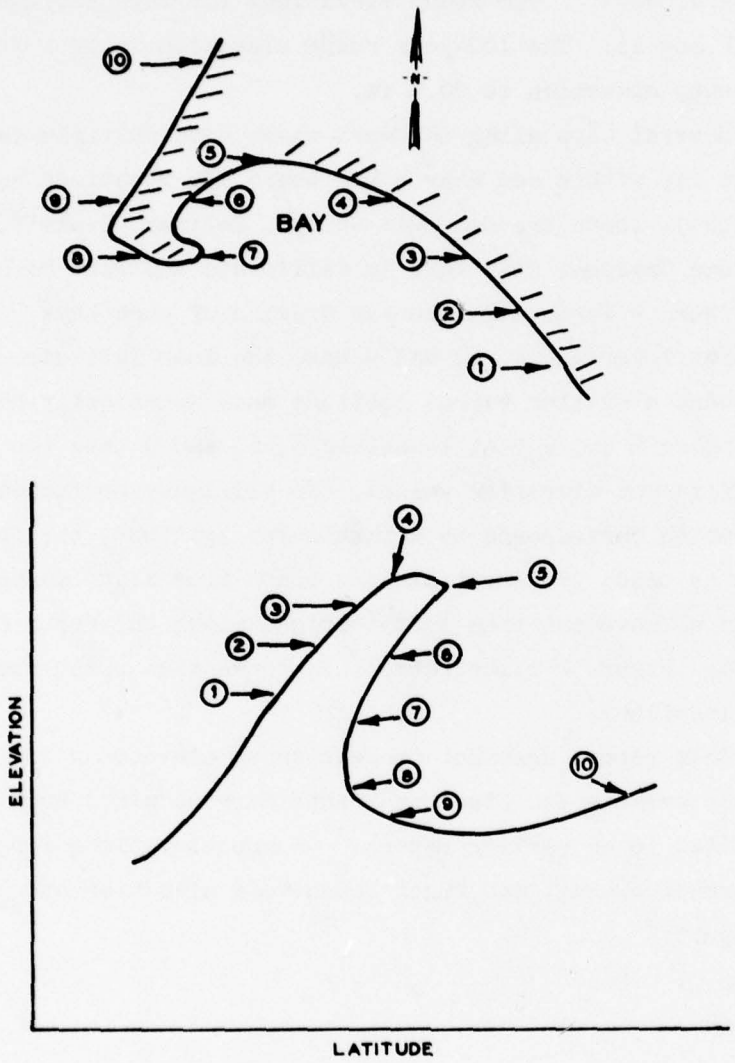

Figure 2. Multiple-valued coastlines

PART III: NUMERICAL MODELS

Background

14. Unlike other areas of the Pacific Ocean such as the Hawaiian Islands, the west coast of the continental United States lacks sufficient data to allow tsunami elevation predictions based upon local historical records of tsunami activity. Virtually all of the west coast is completely without data of tsunami occurrence, even data for the prominent 1964 tsunami. Only a handful of locations have historical data for tsunamis other than the 1964 tsunami. However, the FIA requires information on tsunami elevations for the entire west coast of the continental United States, even for the many locations that have no known historical data of tsunami activity and for coastal areas that are currently not developed (since these areas may be developed in the future).

15. The lack of historical data of tsunami activity on the west coast necessitates the use of numerical models to predict runup elevations. The Aleutian-Alaskan area and the west coast of South America were found in Reference 1 to be the tsunamigenic regions of concern to the west coast of the United States. Both regions have sufficient data on the generation of major tsunamis to allow a statistical investigation of tsunami generation. A numerical model employing a fairly crude grid to cover a large section of the Pacific Ocean was used to generate representative tsunamis and propagate them across the deep ocean. A second numerical model employing a fine grid model was used to propagate tsunamis from the deep ocean over the continental slope and shelf to shore. Previous studies[1,2] used analytical methods to solve one-dimensional linear equations that described the transformation of tsunamis as they propagated from deep water to shore. The two-dimensional numerical model used in this study to propagate tsunamis to shore solved equations that included nonlinear advective terms and bottom stress terms.

16. In this report, only tsunamis of distant origin (at least two

or three tsunami wavelengths away from the west coast) are considered in the analysis. Hammack[3] has shown that near the generation area of a tsunami, details of ground motion during the earthquake and details of the permanent deformation of the seafloor influence the form of the resulting tsunami. Very little is known about the actual time-dependent ground motion during earthquakes generating major tsunamis, and small-scale details of the permanent deformation of the seafloor following earthquakes cannot be predicted in advance. Thus, accurate predictions of the properties of locally generated tsunamis are not possible at this time. However, Hammack[3] has shown that the time-dependent ground motions and small-scale details of the permanent ground deformation produce waves which are not significant far from the source region. Thus, distantly generated tsunamis can be studied only knowing major features of the permanent ground deformation.

17. The probability is not considered very great that a destructive, locally generated tsunami will occur on the west coast of the continental United States. Tsunamis are generally produced by earthquakes having fault movements that exhibit a pronounced "dip-slip," or vertical component of motion. "Strike-slip," or horizontal displacement, fault movements are inefficient generators of tsunamis. Faults on the west coast of the United States characteristically exhibit strike-slip motion since the Pacific block of the earth's crust is moving horizontally relative to the North American block. The west coast of the United States does not share the characteristics (oceanic trenches and island arcs) of known tsunami-generating areas and, in fact, has not historically been one. Relatively small locally generated tsunamis have been known to occur on the west coast, but there are no reliable reports of major locally generated tsunamis. There could be a few locations on the west coast for which locally generated tsunamis pose a greater hazard than do distantly generated tsunamis because the elevations produced by distantly generated tsunamis are small. However, predictions of elevations produced by locally generated tsunamis are beyond the scope of this report.

Generation and Deep-Ocean Numerical Model

18. The finite-difference numerical model used to simulate the generation of tsunamis and their propagation across the deep ocean was originally developed by Hwang et al.,[4] and described in detail in an earlier report.[1] In this study the model employed 1/3° by 1/3° spherical coordinate grids to solve the linearized long-wave equations. Such crude grids adequately resolve the very long tsunami wavelengths in the deep ocean. A comparison of a wave gage recording of the 1964 tsunami at Wake Island in the Pacific Ocean and a simulation of the 1964 tsunami using this numerical model and 1/3° by 1/3° grid verified the accuracy of such a grid spacing.[5] The grids covered very large sections of the Pacific Ocean including either Alaska and the west coast of the United States or South America and the west coast of the United States. The boundary condition on the solid boundaries (land) of the grids was that the component of the velocity normal to the boundary equals zero. On open boundaries (ocean), a first-order approximation of total transmission was made.

19. The deep-ocean finite-difference model solved an initial value problem starting with an uplift deformation of the water surface identical with the major features of the permanent deformation (permanent in the sense that the time scale associated with it is much longer than the period of the tsunami) of the seafloor following the seismic disturbance. The transient movements within the time history of the ground motion were neglected because Hammack[3] has shown that these movements are unimportant in the far field for a spatially large impulsive ground motion. Hammack has further shown that the inital deformation of the water surface will closely approximate major features of the permanent deformation of the ocean floor, provided these features have characteristic lengths that are at least four times as great as the water depth. The neglect of smaller features is unimportant because such small-scale details produce waves that are negligible in the far field.[3]

Nearshore Numerical Model

20. The nearshore finite-difference numerical model[6] was based upon the original formulation of a tidal hydraulics model by Leendertse.[7] The model has been applied in several studies to analyze the tidal hydraulics of harbors and inlets.[8,9] It also has been used to calculate decay of a tsunami as it enters and spreads throughout San Francisco Bay.[2]

21. The fundamental equations solved by this numerical model were vertically arranged and expressed in a Cartesian coordinate system. The momentum equations were

$$\frac{\partial U}{\partial t} + U\frac{\partial U}{\partial x} + V\frac{\partial U}{\partial y} + g\frac{\partial \eta}{\partial x} + \frac{T_B^x}{h + \eta} = 0 \qquad (1)$$

$$\frac{\partial V}{\partial t} + U\frac{\partial V}{\partial x} + V\frac{\partial V}{\partial y} + g\frac{\partial \eta}{\partial y} + \frac{T_B^x}{h + \eta} = 0 \qquad (2)$$

where

$T_B^x = gU/C^2\sqrt{U^2 + V^2}$

$T_B^y = gV/C^2\sqrt{U^2 + V^2}$

T_B^x and T_B^y = bottom stress terms

C = Chezy coefficient

The continuity equation was:

$$\frac{\partial \eta}{\partial t} + \frac{\partial}{\partial x}(h + \eta)U + \frac{\partial}{\partial y}(h + \eta)V = 0 \qquad (3)$$

23. This set of equations was solved by a system of finite-difference equations using central differences on a space-staggered grid. Leendertse's implicit-explicit multioperational method was employed in determining η as a function of time.

24. The nearshore numerical model used as input the time-history calculated by the generation and deep-ocean propagation numerical model. A tsunami was generated in the Aleutian-Alaskan area or the west coast of South America and propagated across the deep ocean to a 500-m depth off the west coast of the United States. Wave forms calculated at this

depth by the deep-ocean numerical model were recorded all along the west coast. These wave forms then were used as input to the nearshore numerical model, which propagated the tsunamis from the 500-m depths across the continental slope and shelf to shore.

25. Figure 3 shows outlines of the four numerical grids used to cover the west coast. The grids had square grid cells 2 miles on a side. The offshore bathymetry was modeled from the 500-m contour to shore. Beyond the 500-m contour, the ocean was modeled as being a constant 500-m depth. The input boundary of each grid was located approximately one and one-half wavelengths of a 30-min wave from the shore. Therefore, at least three typical waves could arrive at the shore before waves were rereflected from the input boundary. The wave forms used as forcing functions varied along the input boundaries in

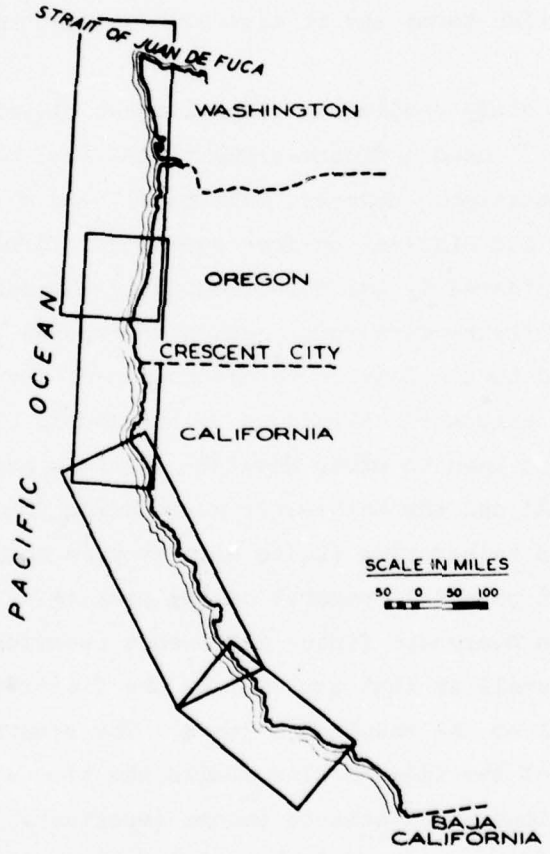

Figure 3. Nearshore grids

accordance with the calculations of the generation and deep-ocean propagation model. The input boundaries of the grids were oriented approximately parallel to the shoreline, since refraction would have bent the wave fronts to such an orientation before they reached the 500-m contour.[10] Lateral boundaries of the grids were impermeable vertical walls.

26. In previous studies,[1,2] an analytical solution was used to propagate tsunamis across the continental slope and shelf to shore. This analytical approach had limitations since it solved a one-dimensional, linear, dissipation-free equation and required the wave form to be sinusoidal and of constant height. The finite-difference model used in this study remedied these limitations since it solved two-dimensional equations that included both nonlinear advective terms and bottom dissipation terms and it also allowed input of arbitrary wave forms.

27. A recent study predicting tsunami runup elevations in the Hawaiian Islands[11,12] used a finite-element numerical model for nearshore tsunami propagation. However, this model used a time-harmonic solution of linear and dissipation-free equations. Arbitrary wave forms could be considered by the model, but only through Fourier decomposition of the arbitrary wave form, separate response calculations for each component, and then a Fourier recomposition of the product of the components and the responses calculated by the model. The finite element approach was used to study Hawaiian tsunamis because these islands are so small and the bathymetry surrounding them is so rapidly varying that only a telescoping finite element grid could adequately represent important physical features of the problem. It would not be feasible for the nearshore finite difference numerical model to use a grid spacing as small as that employed by the finite element model and still cover all of the Hawaiian Islands. The remarkably narrow continental shelf of the islands also limits the time available for nonlinear and dissipative effects to become important. Thus, the finite element model was ideal for studying tsunami interaction with the Hawaiian Islands, but of less value for studying tsunamis on the west

coast of the United States where land-water boundary changes and depth variations are relatively gradual and nonlinear and dissipative effects possibly of greater importance.

Verification

28. The numerical models used in this report were verified by numerical simulations of the 1964 Alaskan tsunami. This was the only large tsunami for which reliable information exists concerning source characteristics. The initial condition used in the generation and deep-ocean propagation numerical model was that the uplift of the ocean's surface in the source region was identical with the permanent deformation of the ocean bottom following the earthquake. The permanent deformation of the ocean's bottom as a function of spatial location was taken from Plafker.[13]

29. Figure 4 shows surface elevation contours approximately 3-1/2 hr after the 1964 Alaskan earthquake, as calculated by the deep-ocean propagation numerical model. This figure illustrates the concentration of energy on the northern California, Oregon, and Washington coasts due to the directional radiation of energy from the source region. The upper section of Figure 5 shows a time-history of the 1964 Alaskan tsunami calculated by the deep-ocean numerical model near Crescent City, California, in a water depth of 500 m. This wave form was used as input to the nearshore propagation numerical model.

30. The lower section of Figure 5 shows a comparison between a tide gage recording of the 1964 tsunami at Crescent City and the nearshore numerical model calculations. The numerical model calculations agree quite well with the tide gage recording. Periods, phases, and amplitudes are in good agreement. The greatest disagreement is the amplitude of the third wave. It should be noted that there is disagreement on the amplitude of the actual historical third and fourth wave crests. Figure 5 shows a reconstruction of the 1964 tsunami at Crescent City inferred by Wilson and Torum[10] from the prototype gage record, and later survey measurements by Magoon.[14] The elevation of the fourth

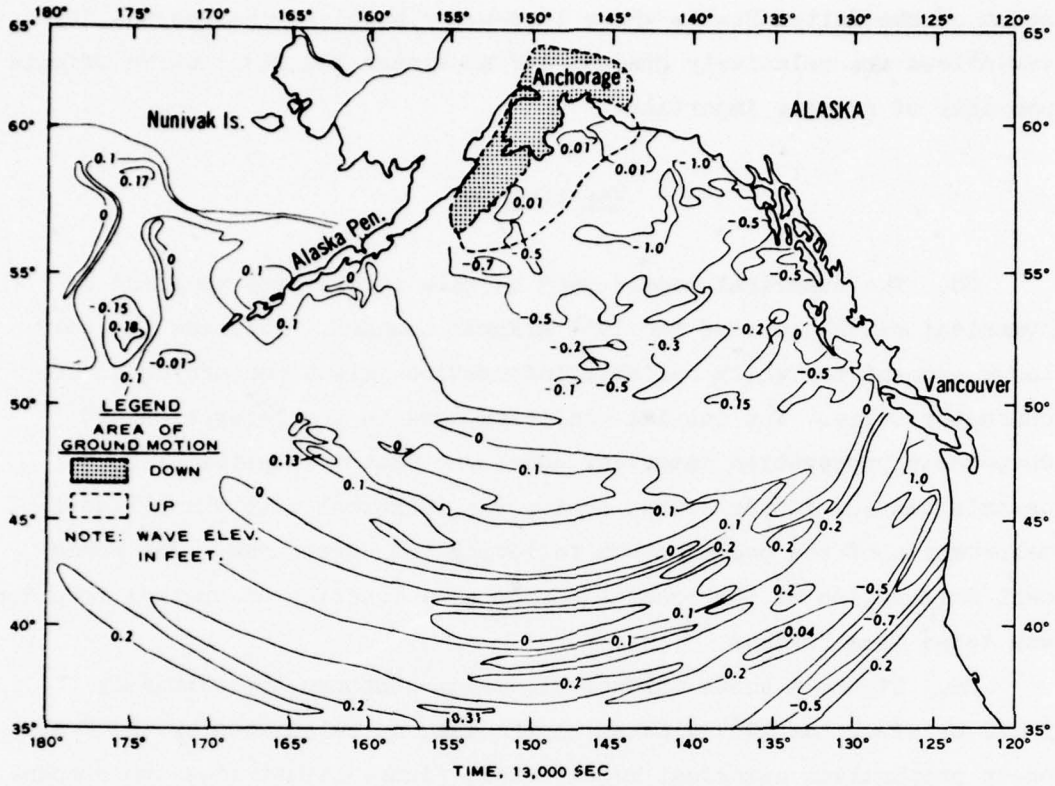

Figure 4. Water-surface elevations 3-1/2 hr after 1964 earthquake (Hwang, 1972)

wave (not shown) was estimated by Wilson and Torum to have been a little less than 14 ft above mean lower low water (mllw). The zero elevation shown in Figure 5 is the mllw datum. Wiegel,[15] however, estimated that the elevation of the third wave was approximately 16 ft above mllw and that the fourth wave attained the highest elevation of 18 or 19 ft above mllw at the tide gage location. The numerical model predicted a fourth wave elevation approximately the same as that estimated by Wilson and Torum (14 ft above mllw). However, reflections from the input boundary were probably growing in importance in the numerical model calculations during the arrival of this fourth wave.

31. There may be several reasons why the maximum wave elevation predicted by the numerical model is not in as good agreement with the historical record as are the elevations of the initial waves. First, the later waves in the deepwater wave form are probably waves which

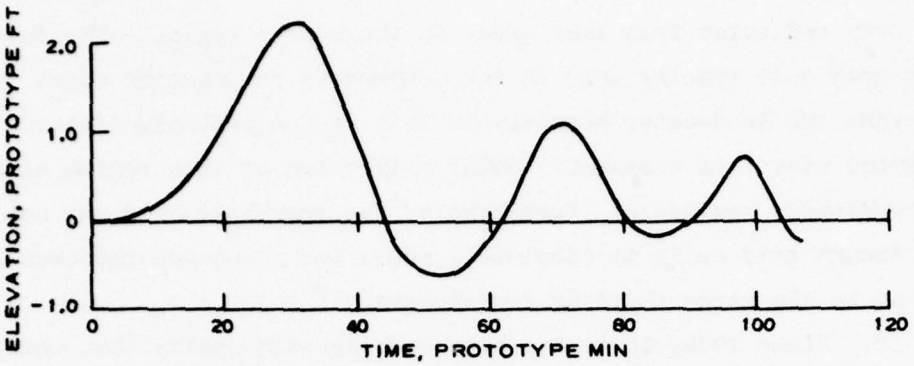

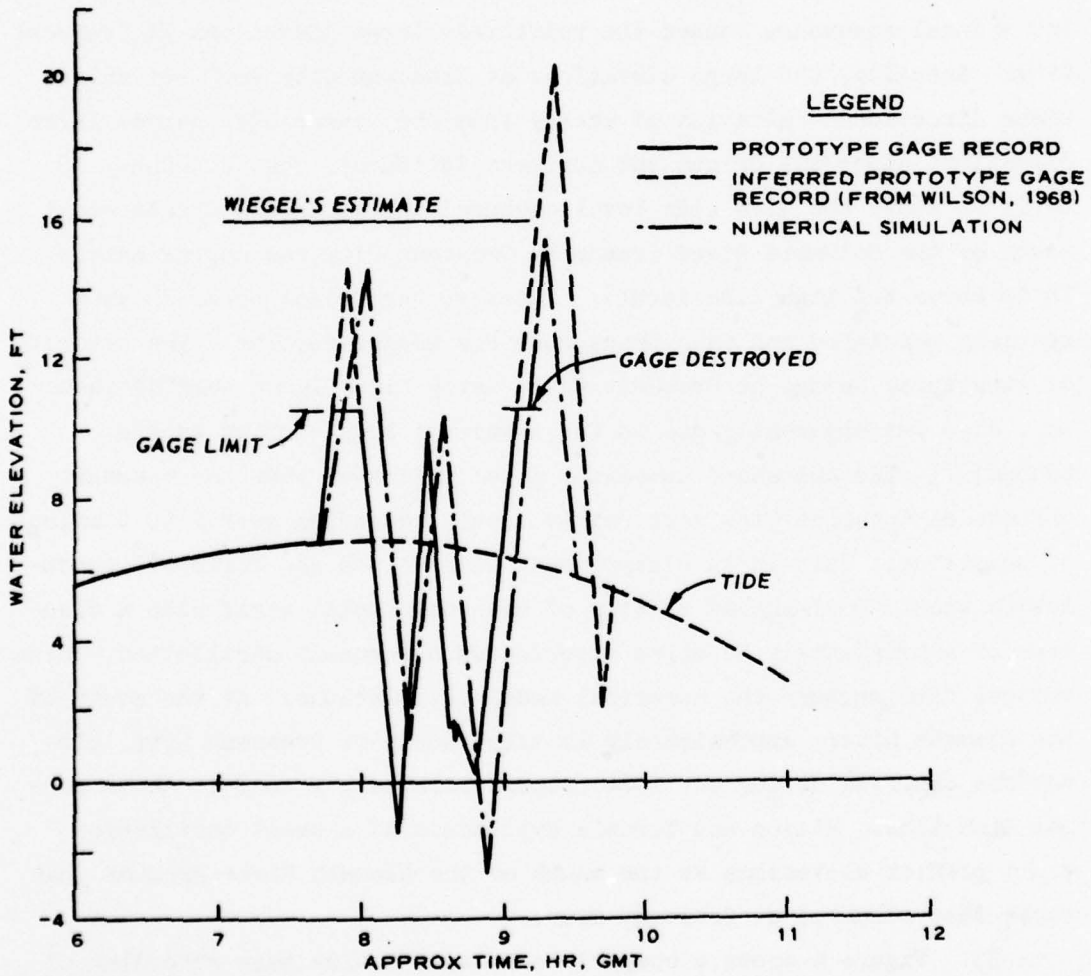

Figure 5. 1964 tsunami at Crescent City, California

have been reflected from land areas in the source region. The fairly large grid cell spacing used in the deep-ocean propagation model to represent the land-water boundary in this region probably distorts the reflected wave form somewhat. Total reflection of this region also was not completely realistic. Furthermore, the nearshore grid may not have fine enough grid cells to completely model the resonance phenomenon leading to the large third or fourth wave.

32. Since 1964, there has been considerable speculation concerning the reasons that the effects of the 1964 tsunami were so great at Crescent City. The finite-difference numerical models showed that both the directional radiation of energy from the source region (Figure 4) and a local resonance caused the relatively large elevations at Crescent City. Actually, the large elevations at Crescent City were not unique since directional radiation of energy from the source also caused large elevations along the Oregon and northern California coasts. Runup 10 to 15 ft above the high tide level occurred all along the Oregon coast south of the Columbia River (runup at Crescent City was approximately 15 ft above the high tide level). However, the Oregon coast is very sparsely populated and thus there were few damage reports. The severity of structural damage at Crescent City, which has a large logging industry, also was apparently due to the impact of logs carried by the tsunami.[10] The nearshore numerical model indicated that the resonant effects at Crescent City were fairly local, extending over 2 to 4 miles of coastline. This is in disagreement with Wilson and Torum's[10] speculation that a bowl-shaped section of the continental shelf with a diameter of approximately 50 miles experienced a resonant oscillation. Historical data support the numerical model calculations. At the mouth of the Klamath River, approximately 15 miles south of Crescent City, elevations observed during the 1964 tsunami were only 2 to 3 ft above normal high tide. Wilson and Torum's hypothesis of a shelf oscillation would predict elevations at the mouth of the Klamath River greater than those that occurred at Crescent City.

33. Figure 6 shows a comparison between a tide gage recording of the 1964 tsunami at Avila Beach, California, and the nearshore model

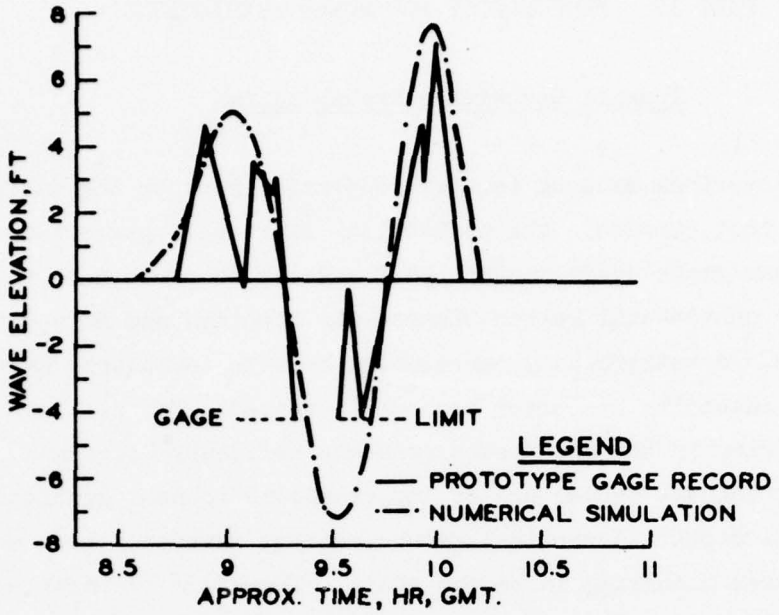

Figure 6. 1964 tsunami from Alaska recorded at Avila Beach, California

calculations. The elevations recorded by the Avila Beach tide gage were larger than those recorded at any tide gage on the west coast except the Crescent City gage. The historical and calculated wave forms shown in Figure 6 are in good general agreement. The tide gage record obviously has higher frequency components not predicted by the numerical model. These components may be local oscillations of water areas which are too small to be accurately represented by the numerical grid. Important features such as the wave amplitudes are in good agreement.

34. The good agreement between the numerical model simulations and tide gage recordings of the 1964 tsunami at the two locations where the largest waves were recorded in 1964 by tide gages verified the numerical techniques described in the previous section. Other tide gage recordings of the 1964 tsunami on the west coast (except at Astoria, Oregon) were in areas not covered by the grids shown in Figure 3 (these areas were considered in References 1 and 2). A comparison with the tide gage at Astoria, Oregon, was not made because Astoria is approximately 12 miles away from the coast in the estuary of the Columbia River. Waves of the 1964 tsunami were small at Astoria.

PART IV: METHODOLOGY FOR RUNUP PREDICTIONS

Tsunami Occurrence Probabilities

35. Historical data on tsunami generation must be the basis for an analysis that considers the probability of tsunami generation in the two tsunamigenic areas in the Pacific Ocean of concern to the west coast of the continental United States--the Aleutian and Peru-Chile Trench areas. A satisfactory correlation between earthquake magnitude and tsunami intensity has never been demonstrated. Not all large earthquakes occurring in the ocean even generate noticeable tsunamis. Furthermore, earthquake parameters of importance to tsunami generation, such as focal depth and vertical ground motion, have only been measured for earthquakes occurring in recent years. Therefore, data on earthquake occurrence cannot be used to determine occurrence probabilities of tsunamis. Historical data of tsunami occurrence in generation regions must be used to determine these probabilities.

36. In South America, a wealth of information exists concerning tsunami occurrence. Reliable data (grouped in intensity increments of 0.5) existed for tsunamis with intensity greater than or equal to 0 for a 169-year period and greater than or equal to 2.5 for a 417-year period. The intensity scale used was a modification (by S. L. Soloviev of the Soviet Union) of the standard Imamura-Iida tsunami intensity scale. Intensity is defined as

$$i = \log_2 (\sqrt{2}\, H_{avg})$$

This definition in terms of an average runup (in metres) over a coast instead of a maximum runup elevation at a single location (used for the standard Imamura-Iida scale) tends to eliminate a spurious intensity magnitude caused by often observed anomalous responses (due, for example, to local resonances) of single isolated locations.

37. Using the most recent and complete catalog of tsunami occurrence in the Pacific Ocean,[16] a relation between tsunami intensity

and frequency of occurrence was determined for the tsunami-generating trench running the length of the Peru-Chile coast. Tsunamis with intensity greater than or equal to 0 were considered. It was assumed that the logarithm of the tsunami frequency of occurrence was linearly related to the tsunami intensity. Earthquake magnitude and frequency of occurrence have been similarly related by Gutenberg and Richter[17] and used extensively in earthquake predictions. Soloviev[18] has shown a similar relation between tsunami intensity and frequency of generation for moderate to large tsunamis throughout the Pacific Ocean. Furthermore, Wiegel[15] found the same type of relation between tsunami occurrence and runup levels for historical tsunamis at Hilo, Hawaii; San Francisco, California; and Crescent City, California; and Adams[19] for tsunamis at Kahuku Point, Oahu. A recent study by Rascon and Villarreal[20] revealed this same relation for historical tsunamis on the west coast of Mexico (data from 1732) and on the Pacific west coast of North America, excluding Mexico.

38. Letting $n(i)$ equal the probability of a tsunami with an intensity i being generated during any given year and using statistics for the entire trench along the Peru-Chile coast, a least-squares analysis resulted in the following expression:

$$n(i) = 0.074e^{0.63i}$$

39. In using statistics for the entire trench area along the Peru-Chile coast, it was assumed that the probability of tsunami occurrence was uniform along the trench. This is a standard assumption for earthquake frequency analysis.[17] The tectonic justification of this assumption lies in the fact that a single sialic block or plate of the earth's crust or lithosphere is dipping into the Peru-Chile Trench.[21] It can be reasonably expected that the movement of this single plate is similar along its entire length.

40. In the Aleutian Trench area, only large tsunamis occurring in relatively recent years (since 1788) have been recorded due to the isolation of the area. Assuming an exponential coefficient of -0.71

for this trench area (determined in Reference 18 as a mean value for areas of the Pacific with the most data on tsunamis) and using only the reliable data for large tsunamis (intensity greater than or equal to 3.5, Reference 16), the following relation was determined by a least-squares analysis:

$$n(i) = 0.113e^{-0.71i}$$

Again, the probability of tsunami occurrence was assumed to be uniform along the trench.

Use of Numerical Models

41. To relate the probability distribution of tsunami intensities to source characteristics, it was assumed that the ratio of the source uplift heights producing two tsunamis of different intensities (as defined in the previous section) is equal to the ratio of the average runup heights produced on the coasts near these tsunami sources. This ratio is equal to $2^{(i_1-i_2)}$ for two tsunamis with intensities i_1 and i_2.

42. If H_a is the wave height emitted in the direction parallel to the major axis of length a by a tsunami source with an elliptical shape (large tsunamis have historically had elliptically shaped uplifts) and H_b is the wave height emitted in the direction parallel to the minor generation axis of length b, then experimental research of tsunami generation has shown that $H_b/H_a \simeq a/b$ (Reference 22). For a large tsunami, H_b can be larger than H_a by a factor of as much as 5 or 6. Thus, the orientation of the tsunami source relative to the area where runup is to be determined is very important; that is, the runup at a distant site due to the generation of a tsunami at one location along a trench cannot be considered as being representative of all possible placements of the tsunami source in the entire trench region. Hence, the Aleutian and Peru-Chile Trenches had to be segmented and runup along the west coast of the United States determined for tsunami

sources located at the center of each of the segments.

43. The spatial size of a tsunami source was standardized because there is not an apparent correlation between tsunami intensity and spatial size of a tsunami source. For example, the 1946 Aleutian tsunami had an uplift region of very small spatial extent, whereas the 1957 Aleutian tsunami had an uplift region that covered perhaps the greatest spatial extent of any known earthquake;[23] yet the 1946 tsunami had the greater intensity, producing, in general, greater runup elevations in the near and distant regions.

44. A description of the standard source employed, given in Reference 1, represents a large tsunami with intensity 4 on the modified Imamura-Iida scale. Certainly, tsunamis of low intensity may have smaller spatial extents; however, large tsunamis pose the greatest threat to a distant area such as the west coast of the United States. These large tsunamis can be expected to have similar spatial extents, with any spatial differences being unimportant in the far field compared with the effects of source orientation and vertical uplift.

45. Figures 7 and 8 show the Aleutian Trench divided into 12 segments and the Peru-Chile Trench into 3 segments. The segments in the Aleutian Trench were approximately one-quarter the length of the major axis of the standard source, whereas the segments in the Peru-Chile Trench were approximately the length of the major axis of the standard source. The standard source was centered in each segment such that the major axis of the source was parallel to the trench axis. Uplift regions historically have had such an orientation relative to trench systems. The Aleutian Trench was segmented much finer than the Peru-Chile Trench because the Aleutian Trench is oriented relative to the west coast such that elevations produced on the west coast are very sensitive[24] to the location of a source along the Trench. Uplifts along the Peru-Chile Trench do not radiate energy directly toward the west coast regardless of their position along the Trench. The Peru and Chile sections of the Peru-Chile Trench have constant orientations relative to the west coast of the United States; therefore elevations

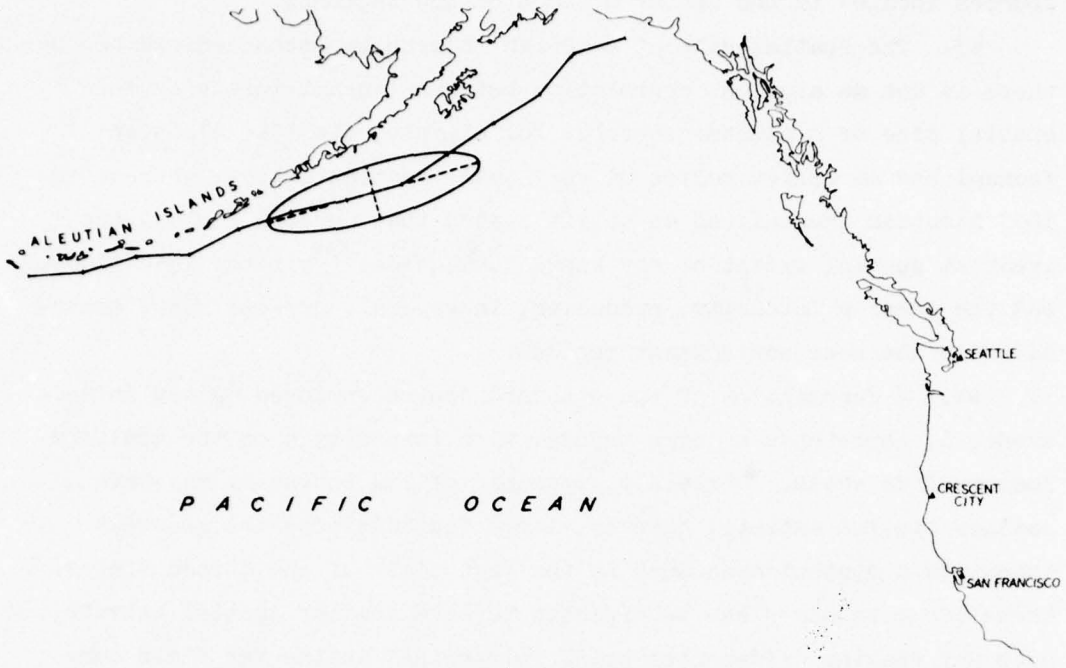

Figure 7. Idealized axis of Aleutian Trench showing 12 segments and perimeter of standard uplift area

on the west coast are not very sensitive[25] to source location within these sections.

46. In each of the segments of the Aleutian and Peru-Chile Trenches, tsunamis with intensities from 2 to 5 in increments of 0.5 were generated and propagated across the deep ocean using the deep-ocean numerical model discussed in an earlier section. Tsunamis with intensity less than 2 are too small to produce significant runup on the west coast. An upper limit of 5 was chosen because the largest tsunami intensity ever reported was less than 5.[16] Reference 17 indicates that there is an upper limit to the strain which can be supported by rock before fracture. Thus, earthquakes only reach certain maximum magnitudes and tsunamis can be expected to have similar upper limits of intensity. Perkins[26] and McGarr[27] have demonstrated that future earthquakes cannot have seismic moments (measure of earthquake magnitude for large earthquakes) much larger than those of earthquakes that occurred in recorded history.

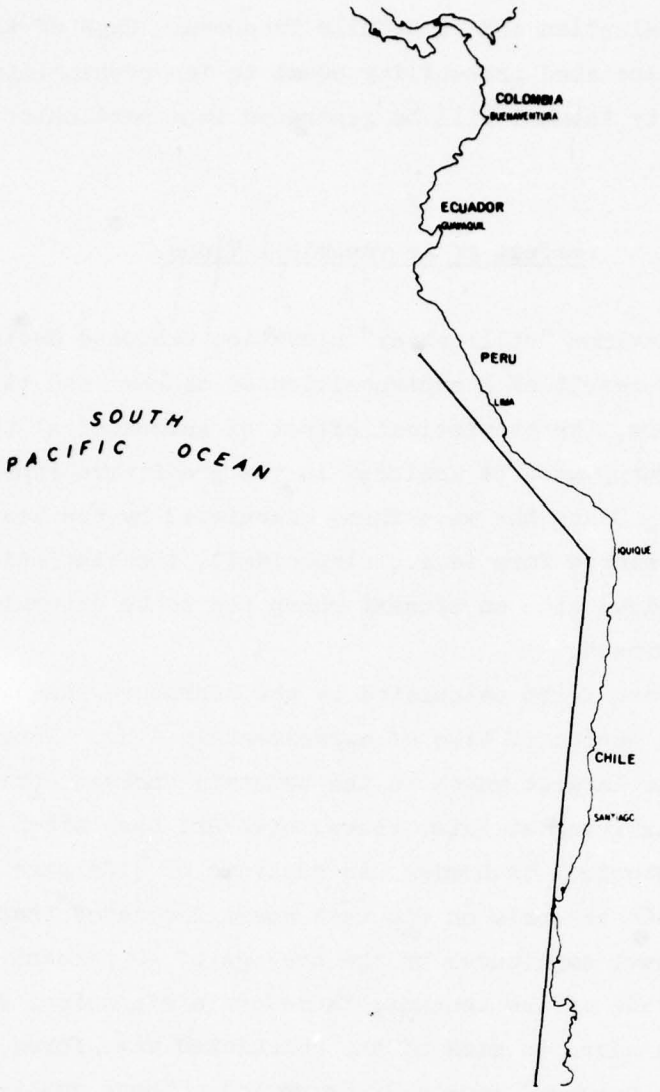

Figure 8. Idealized axis of Peru-Chile Trench showing 3 segments

47. The wave forms propagated to the west coast by the deep-ocean propagation numerical model were used as input to the nearshore propagation numerical model. Each wave form was propagated from a water depth of 500 m to shore using the nearshore model and one of the grids shown in Figure 3. Thus, at each grid location on the shoreline of the west coast, there was a group of 105 wave forms--seven wave forms (for intensities from 2 to 5 in increments of 0.5) for each

segment of the Aleutian and Peru-Chile Trenches. Each of these wave forms had an associated probability equal to the probability that a certain intensity tsunami will be generated in a particular segment of a trench region.

Effect of Astronomical Tides

48. The maximum "still water" elevation produced during tsunami activity is the result of a superposition of tsunami and tidal wave forms. Therefore, the statistical effect of astronomical tides on total tsunami runup must be included in the predictive scheme presented in this report. Since the wave forms calculated by the nearshore model did not have a simple form (e.g., sinusoidal), the statistical effect of the astronomical tide on tsunami runup had to be determined through a numerical approach.

49. The wave forms calculated by the nearshore numerical model extended over a period of time of approximately 2 hr. Three or four wave crests (the largest waves in the tsunami) arrived during this time. Smaller waves arriving at later times, however, have often persisted for days during historical tsunamis. An analysis of tide gage records of the 1960 and 1964 tsunamis on the west coast indicated that these smaller waves have amplitudes on the average of 40 percent of the maximum wave amplitude of the tsunami; therefore a sinusoidal group of these small waves was added to each of the calculated wave forms so that the total wave form extended over a 24-hr period. These smaller waves are important for locations where tsunami waves are fairly small compared with tidal variations. At such locations, the maximum combined tsunami and astronomical elevation occurs during the maximum tidal elevation.

50. A computer program was developed to predict time-histories of the astronomical tides at all grid locations on the west coast of the United States. The program was based upon the harmonic analysis methods used in the past by the National Ocean Survey for mechanical tide-predicting machines.[28] Tidal constants available from the National Ocean Survey were used as input to the computer program. A year of

tidal elevations was then predicted for grid locations all along the west coast. The year 1964 was selected because all the major tidal components had a node factor of approximately 1.00 during this year, thus making it an average year. The node factor is associated with the revolution of the moon's node and has an 18.6-year cycle. Since a tsunami can arrive at any time during this 18.6-year period (arrival at a low of the node factor is equally likely as an arrival at a high), the statistical effect of the varying node factor is small and an average value should be used. The statistical effect of the varying node factor on the predicted runup elevations can be shown to be a small fraction of an inch using the approach discussed in paragraphs 56 and 57 (with a σ for the nodel variation approximately equal to 0.5 in. squared).

51. The tidal time-histories calculated at each of the nearshore numerical model grid points along the west coast were then subdivided into 15-min segments. Each of the 105 24-hr wave forms was allowed to arrive at the beginning of each of these 15-min segments and then superimposed upon the astronomical tide for the 24-hr period. The maximum combined tsunami and astronomical tide elevation over the 24-hr period was determined for tsunami wave forms arriving during each of these 15-min starting times. Each of these maximum elevations had an associated probability equal to the probability that a certain intensity tsunami would be generated in a particular segment of the two trench regions and arrive during a particular 15-min period of a year.

52. The many maximum elevations with associated probabilities were used to determine cumulative probability distributions of combined tsunami and astronomical tide elevations. The maximum elevations were ordered and probabilities summed, starting with the largest elevations, until a desired probability was obtained. The elevation encountered when the summed probabilities reach a desired value P was the elevation that is equaled or exceeded with an average frequency of once every $1/P$ years. Thus, when the summed probabilities reached the value 0.01, the elevation associated with the last probability summed was the 100-year elevation.

53. 100- and 500-year elevations were determined at all grid points of the nearshore numerical grids. Smooth curves were then used to connect all these discrete elevations, resulting in the continuous elevation curves shown in Plates 1-30.

Comparison with Local Observation Predictions

54. Crescent City, California, was the only location on the portion of the west coast of the United States considered in this report (that is, the west coast minus Southern California, Monterey Bay, San Francisco Bay, and Puget Sound) which had sufficient historical data of tsunami activity to allow frequency of occurrence predictions based upon local historical observations (note, however, discussion for San Francisco in next section). Wiegel[15] made such predictions of tsunami height (trough to crest height) for the period from 1900 to 1965. He predicted 100- and 500-year heights at Crescent City of approximately 25.6 ft and 43.2 ft (extending his curve) respectively. If the crest amplitude is taken to be one-half the total height, the 100- and 500-year elevations are 12.8 ft and 21.6 ft, respectively. However, the crest amplitude at Crescent City is typically greater than one-half the wave height (e.g., the crest amplitude of the largest wave of the 1964 tsunami was approximately 60 percent of the total height). If Wiegel's analysis is applied to historical crest elevations instead of heights, the 100- and 500-year elevations are found to be 15.4 ft and 26.4 ft, respectively. Furthermore, the analysis now can be applied to the longer time period from 1900 through 1977. The 100- and 500-year elevations based upon this longer time span are 14.5 ft and 25.5 ft, respectively.

55. Plate 17 shows 100- and 500-year elevations at Crescent City of 13.1 ft and 24.9 ft, respectively. These values compare very favorably with the 14.5- and 25.5-ft elevations determined from historical data for the period of time from 1900 through 1977. The elevations predicted by the analysis based upon the local historical data are probably somewhat larger than the elevations predicted in this report because the

short time period (relative to 100 and 500 years) from 1900 through 1977 includes the exceptionally active years of tsunami generation from 1946 through 1964. The three greatest intensity tsunamis generated in the Aleutian-Alaskan region since at least 1788 occurred during this time span. The 1960 Chilean tsunami was the greatest intensity tsunami generated in the Peru-Chile region since at least 1562.

56. The 13.1- and 24.9-ft elevations predicted for Crescent City using the techniques discussed in this report are not quite comparable to the elevations predicted using Wiegel's analysis based upon local historical data because the effect of the astronomical tide has been included in the elevations predicted in this report but not in Wiegel's analysis. However, the statistical effect of the astronomical tide on the tidal elevation is small at Crescent City because tsunamis are so large. Reference 1 shows that statistical effect of the astronomical tide for a location where tsunami waves are large (so that one wave is much larger than any other) is to increase the predicted elevation by an amount equal to

$$\frac{\alpha\sigma^2}{2}$$

where σ^2 is the tidal variance and equals

$$\sum_{m=1}^{\infty} C_m^2$$

where C_m is equal to the m^{th} tidal constituent.

57. The term α is given by the following expression:

$$P(Z) = Ae^{-\alpha Z}$$

where

A = constant coefficient

Z = the runup at any time above local mean sea level

$P(Z)$ = the cumulative probability distribution for runup at a given site being equal to or exceeding Z due only to the maximum wave of the tsunami.

This form of the probability distribution is well established for tsunamis (see paragraphs 35-40).

58. Based upon the tidal constituents predicted by the National Ocean Survey, $\sigma^2 = 7.1$ for Crescent City. Using Wiegel's data, the period of time from 1900 through 1977 gives $\alpha = 0.145$. Therefore, the astronomical tide contributes approximately 0.5 ft to the elevations predicted for Crescent City.

San Francisco Elevation Predictions

59. Frequency of occurrence calculations for San Francisco Bay were made in an earlier report[2]; however, a large section of San Francisco Bay was included in the nearshore numerical model grid (Figure 3) used in this study in order that the effect of the bay on elevations outside the bay could be properly simulated. Thus, elevation calculations were made in this study at the location of the Presidio tide gage in San Francisco Bay. Plate 9 shows the 100- and 500-year elevation predictions at this location to be 6.1 ft and 10.0 ft, respectively. Reference 2 predicted elevations of 8.0 and 15.5 ft near the Presidio tide gage. However, the simple one-dimensional nearshore solution employed in Reference 2 could only propagate the leading wave of the tsunami to a location near the mouth of San Francisco Bay and then it had to be assumed that the elevation at the Presidio tide gage was the same as this calculated elevation. Thus, the elevations predicted for the tide gage in Reference 2 really are elevations for San Francisco just outside the bay; consequently, the elevations predicted in Reference 2 at the Presidio tide gage and throughout the bay were too large. However, the percentage error in elevations for the interior of San Francisco Bay will be less than the percentage error for the Presidio tide gage, since tsunami elevations are smaller in the bay and, consequently, the effect of the astronomical tides proportionately greater. In fact, for much of San Francisco Bay the error in the tsunami elevation would probably be so small compared with the contribution from the astronomical tide that it would be negligible. If the reduction of a predicted elevation in San Francisco Bay by a percentage equal to the

percentage error at the Presidio tide gage would have a significant impact on a development, then recomputations based upon the results of this study might be warranted.

60. There are sufficient historical data at the Presidio tide gage in San Francisco to make elevation predictions based upon local historical data. Using a logarithmic distribution and Wiegel's wave-height data for San Francisco over the period 1900 through 1977 yields 100- and 500- year heights (trough to crest) of 8.0 ft and 14.2 ft, respectively. If the crest amplitude is one-half the height, this yields 100- and 500-year elevations of 4.0 ft and 7.6 ft, respectively. A similar analysis just based upon historical crest amplitudes (with no assumption concerning the crest to trough ratio) yields 100- and 500-year elevations of 4.4 ft and 7.8 ft, respectively.

61. It is difficult to compare the elevations predicted using local historical data with the elevations of 6.1 and 10.0 ft calculated in this report, because the effect of the astronomical tides (contained in the calculations of this report) cannot easily be estimated, as was the case for Crescent City. Tsunamis recorded at the Presidio tide gage in San Francisco are known to persist at fairly substantial levels for extended periods of time, apparently due to some oscillation phenomenon. For example, during the 1964 tsunami there were six waves of approximately equal or greater amplitude than the initial wave (in addition to smaller waves) during the first 8 hr of the tsunami. Oscillations approximately 40 percent of the amplitude of the initial wave persisted for at least another 24 hr. The tide range at San Francisco is 5.7 ft with mean higher high water (mhhw) 2.7 ft above msl and mean high water (mhw) 1.0 ft above msl. At least one of the main waves of a tsunami at San Francisco probably superimposes upon either mhw (with the smaller oscillations then adding on to mhhw) or mhhw. Thus, the effect of the tides is probably to contribute 1 to 2.7 ft to the total elevation. The average of these tidal elevations is 1.85 ft and if this elevation is added to the 4.4- and 7.8-ft elevations based upon local historical data, the resulting elevations of 6.25 and 9.65 ft are similar to the 6.1- and 10.0-ft elevations calculated in this report.

PART V: CONCLUSIONS AND RECOMMENDATIONS

Conclusions

62. The deep-ocean and nearshore numerical models used in this report accurately simulated tsunami generation, deep-ocean and nearshore propagation, and interaction with coastlines. The nearshore numerical model was superior to the analytical techniques used for nearshore propagation in previous studies (References 1 and 2) at the U. S. Army Engineer Waterways Experiment Station (WES) because it was two-dimensional, solved equations which included nonlinear advective terms and bottom stress terms, and handled arbitrary incident wave forms. It may be advisable to use the nearshore numerical model to recompute elevations for the areas considered in References 1 and 2. However, since the elevations computed in these earlier studies were in general not very large (because the areas considered were protected from tsunamis), there may not be a need for the refinement in nearshore calculations provided by the nearshore numerical model. Nonlinear and bottom stress effects also are less important for smaller tsunamis. Thus, neglect of these effects in References 1 and 2 probably was not generally significant.

63. The techniques (which are based upon historical data from source regions and numerical model calculations) used in this report to predict tsunami runup provided good estimates of 100- and 500-year runup levels for the west coast of the continental United States. The 100- and 500-year predictions at Crescent City and San Francisco, California, based upon the techniques presented in this report, were shown to agree quite well with predictions based upon historical observations of tsunami activity at these two locations. These were the only locations along the coastline considered in this report which had sufficient local historical data to allow predictions based upon local observations.

Recommendations

64. The runup elevations predicted in this report can be assumed

to equal the tsunami shoreline elevation for most of the shoreline presented in Plates 1-30. The similarity between runup elevations and elevations at the shoreline is illustrated in the detailed surveys of tsunami inundation that have been performed following historical tsunamis. For example, Magoon[14] reported flooding to about the 20-ft contour above mllw and elevations at the shoreline of about 20 ft (mllw) for the 1964 tsunami at Crescent City, California. Wilson and Torum[10] reported that the 20-ft (mllw) runup at Valdez, Alaska, for the 1964 tsunami checked "well for consistency with water level measurements made on numerous buildings throughout the town." Similar comments were made by Brown[29] in reference to survey measurements of 30-ft (mllw) runup at Seward, Alaska, for the 1964 tsunami. Runup and elevation at the shoreline were similar at nine locations in Japan as recorded by Nasu[30] in surveys following the 1933 Sanriku tsumani. Runup and elevation at the shoreline were also similar for the borelike waves at Hilo, Hawaii, during the 1960 tsumani.[31]

65. There are locations where time-dependent effects (for example, lack of sufficient time to completely flood extensive low-lying or estuarine areas) or two-dimensional effects (for example, flow divergence or convergence) cause tsunami runup elevations not to be equal to elevations at the shoreline. It is recommended that for these areas inundation limits be determined using a numerical model developed recently at WES.[32] This model is capable of handling land flooding for bays, harbors, developed areas such as cities, large low-lying areas, sand-dune protected areas, and other areas where there are topographical, roughness, or coastline variations.

REFERENCES

1. Houston, J. R. and Garcia, A. W., "Type 16 Flood Insurance Study: Tsunami Predictions for Pacific Coastal Communities," Technical Report H-74-3, May 1974, U. S. Army Engineer Waterways Experiment Station, CE, Vicksburg, Miss.

2. Garcia, A. W. and Houston, J. R., "Type 16 Flood Insurance Study: Tsunami Predictions for Monterey and San Francisco Bays and Puget Sound," Technical Report H-75-17, Nov 1975, U. S. Army Engineer Waterways Experiment Station, CE, Vicksburg, Miss.

3. Hammack, J. L., Jr., "Tsunamis--A Model of Their Generation and Propagation," Report No. KH-R-28, Jun 1972; W. M. Keck Laboratory of Hydraulics and Water Resources, California Institute of Technology, Pasadena, Calif.

4. Hwang, L. S., Butler, H. L., and Divoky, D. J., "Tsunami Model: Generation and Open-Sea Characteristics," Bulletin of the Seismological Society of America, 62, No. 6, pp 1579-1596.

5. Houston, J. R., et al., "Probable Maximum Tsunami Runup for Distant Seismic Events, Islote Site, Puerto Rico," 1975, Fugro Inc., Long Beach, Calif.

6. Houston, J. R. and Garcia, A. W., "Tsunami Elevation Predictions from Numerical Models," American Society of Civil Engineers Annual Convention, Oct 1977, San Francisco, Calif.

7. Leendertse, J. J., "Aspects of a Computational Model for Long-Period Water-Wave Propagation," RM-5294-PR, The Rand Corp., 1967.

8. Raney, D. C., "Numerical Analysis of Tidal Circulation for Long Beach Harbor: Existing Conditions and Alternate Plans for Pier J Completion and Tanker Terminals," Miscellaneous Paper H-76-4, Report 1, Sep 1976, U. S. Army Engineer Waterways Experiment Station, CE, Vicksburg, Miss.

9. _____, "Numerical Analysis of Tidal Circulation for Long Beach Harbor: Tidal Circulation Velocity Patterns for Existing Conditions and Alternate Master Plan Pier J Configurations for SOHIO Project," Miscellaneous Paper H-76-4, Report 2, Mar 1976, U. S. Army Engineer Waterways Experiment Station, CE, Vicksburg, Miss.

10. Wilson, B. W. and Torum, A., "The Tsunami of the Alaskan Earthquake, 1964: Engineering Evaluation," Technical Memorandum No. 25, May 1968, U. S. Army Coastal Engineering Research Center, CE, Washington, D. C.

11. Houston, J. R., Carver, R. D., and Markle, D. G., "Tsunami-Wave Elevation Frequency of Occurrence for the Hawaiian Islands," Technical Report H-77-16, Aug 1977, U. S. Army Engineer Waterways Experiment Station, CE, Vicksburg, Miss.

12. Houston, J. R., "Interaction of Tsunamis with the Hawaiian Islands Calculated by a Finite-Element Numerical Model," Journal of Physical Oceanography, Vol 8, No. 1, Jan 1978.

13. Plafker, G., "Tectonics of the March 27, 1964, Alaska Earthquake," U. S. Geological Survey Professional Paper 543-I, pp. 11-174.

14. Magoon, O. T., "Structural Damage by Tsunamis," Proceedings, American Society of Civil Engineers, Specialty Conference on Coastal Engineering, Santa Barbara, Calif., Oct 1965, pp 35-68.

15. Wiegel, R. L., "Protection of Crescent City, California, from Tsunami Waves," Prepared for the Redevelopment Agency of the City of Crescent City, 1965, Berkeley, Calif.

16. Soloviev, S. L. and Go, Ch. N., "Catalog of Tsunamis in the Pacific (Main Data)," 1969, Union of Soviet Socialist Republics, Moscow.

17. Gutenberg, B., and Richter, C. F., Seismicity of the Earth and Associated Phenomena, 2d ed., 1965, Hafner Publishing Co., New York.

18. Soloviev, S. L., "Recurrence of Tsunamis in the Pacific," Tsunamis in the Pacific Ocean, ed. W. M. Adams, East-West Center Press, Honolulu, 1970.

19. Adams, W. M., "Tsunami Effects and Risk at Kahuku Point, Oahu, Hawaii," Engineering Geology Case Histories, Geological Society of America, No. 8, 1970.

20. Rascon, O. A. and Villarreal, A. G., "On a Stochastic Model to Estimate Tsunami Risk," Journal, Hydraulic Research, Vol 13, No. 4, 1975, pp 383-403.

21. Wilson, B. W., "Earthquake Occurrence and Effects in Ocean Areas," CR 69.027., 1969, Naval Civil Engineering Laboratory, Port Hueneme, Calif.

22. Hatori, T., "Directivity of Tsunamis," Bulletin of the Earthquake Research Institute, University of Tokyo, Vol 41, 1963, pp 61-81.

23. Kelleher, J., et al., "Why and Where Great Thrust Earthquakes Occur Along Island Arc," Journal of Geophysical Research, Vol 79, No. 32, Nov 1974, pp 4889-4899.

24. Houston, J. R., et al., "Effect of Source Orientation and Location in the Aleutian Trench on Tsunami Amplitude Along the Pacific Coast of the Continental United States," Research Report H-75-4, July 1975, U. S. Army Engineer Waterways Experiment Station, CE, Vicksburg, Miss.

25. Garcia, A. W., "Effect of Source Orientation and Location in the Peru-Chile Trench on Tsunami Amplitude Along the Pacific Coast of the Continental United States," Research Report H-76-2, Sep 1976, U. S. Army Engineer Waterways Experiment Station, CE, Vicksburg, Miss.

26. Perkins, D., "The Search for Maximum Magnitude," National Oceanic and Atmosphere Administration Earthquake Information Bulletin, Jul 1972, pp 18-23.

27. McGarr, A., "Upper Limit to Earthquake Size," Nature, Vol 262, Jul 1976, pp 378-379.

28. Schureman, P., Manual of Harmonic Analysis and Prediction of Tides, U. S. Coast and Geodetic Survey, Spec. Pub. No. 98, 1958.

29. Brown, D. L., "Tsunami Activity Accompanying the Alaskan Earthquake, 27 March 1964," U. S. Army Engineer District, Alaska, Apr 1964, Anchorage, Alaska.

30. Nasu, N., "Heights of Tsunamis and Damage to Structures," Bulletin of the Earthquake Research Institute, Supplementary Vol 1, Tokyo Imperial University, 1934, pp 218-235.

31. Eaton, J. P., Richter, D. H., and Ault, W. U., "The Tsunami of May 23, 1960, on the Island of Hawaii," Bulletin of the Seismological Society of America, Vol 51, No. 2, Apr 1964, pp 135-157.

32. Houston, J. R. and Butler, H. L., "A Numerical Model for Tsunami Inundation" (in preparation).

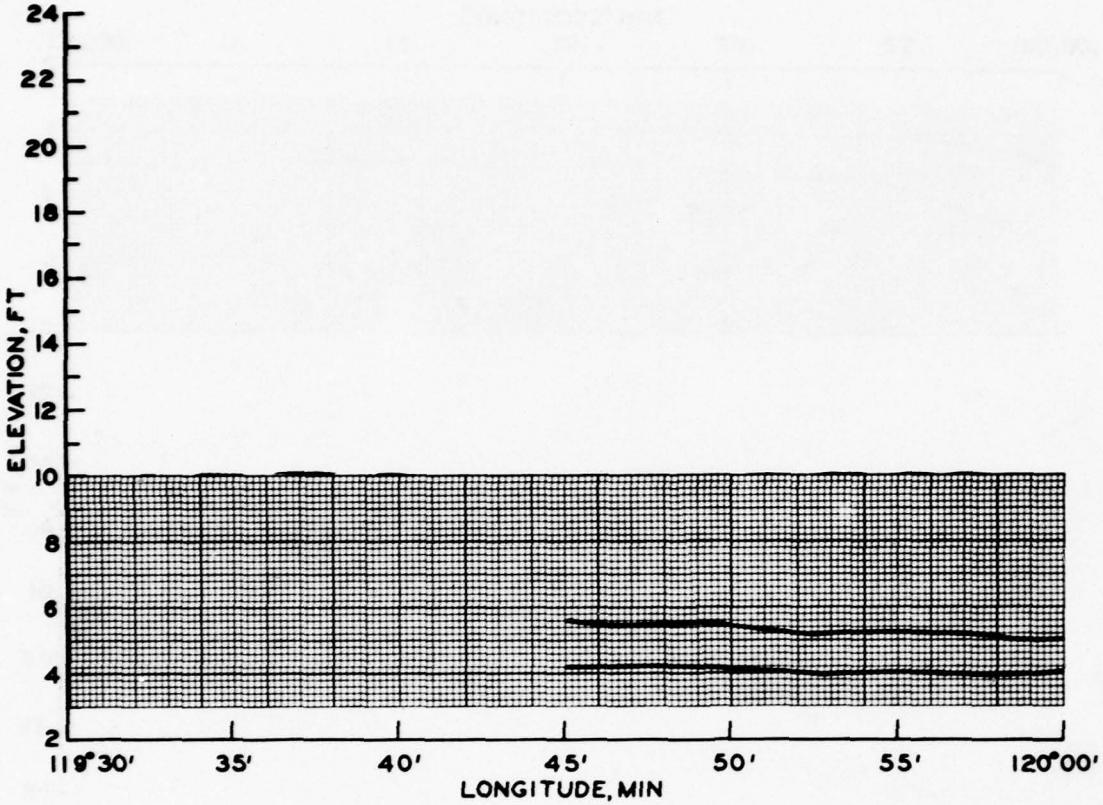

100- AND 500-YEAR ELEVATIONS VS LOCATION

LONGITUDE 119°45' TO 120°00'

PLATE 1

PLATE 2

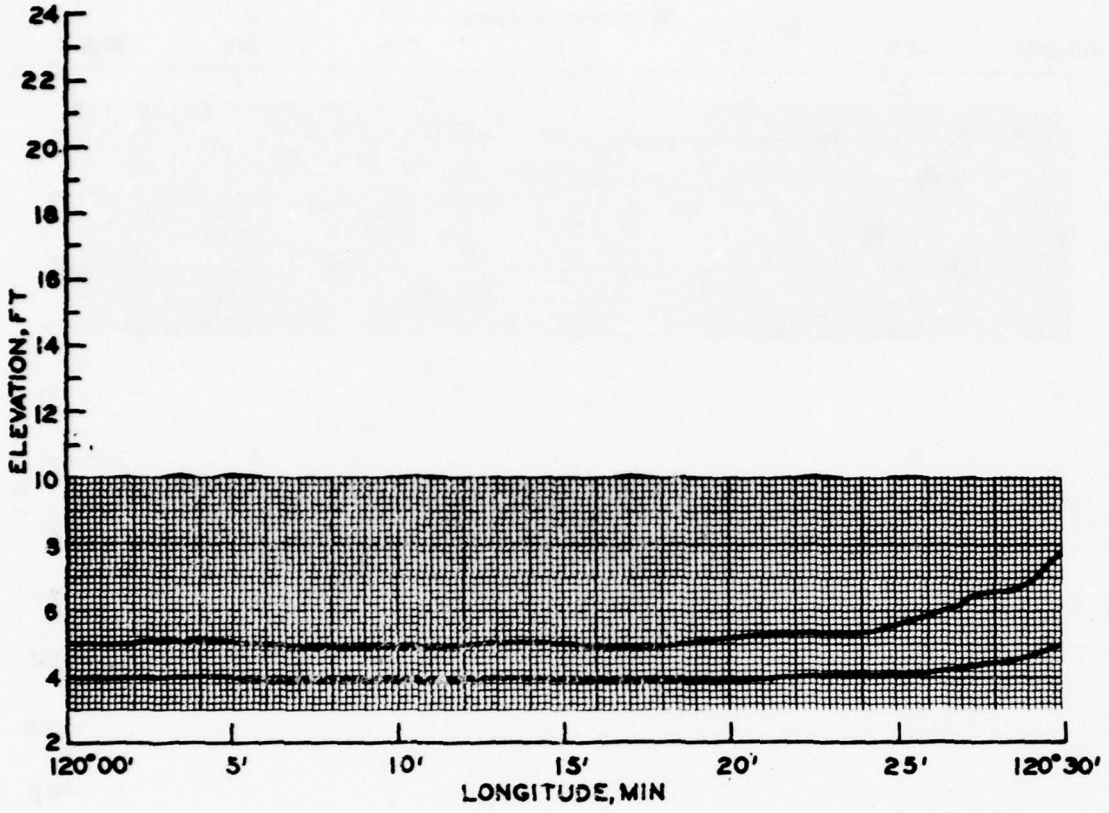

100- AND 500-YEAR ELEVATIONS VS LOCATION

LONGITUDE 120°00' TO 120°30'

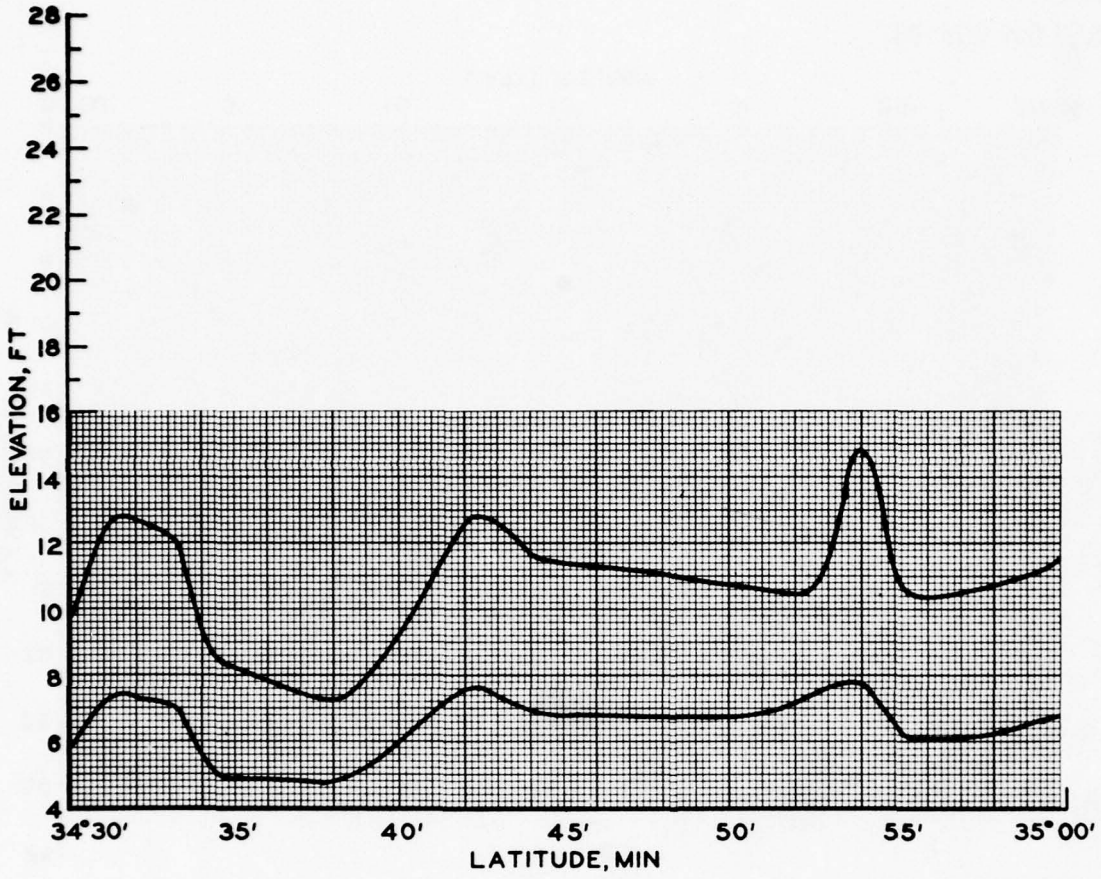

100- AND 500-YEAR ELEVATIONS VS LOCATION

LATITUDE 34°30′ TO 35°00′

PLATE 3

PLATE 4

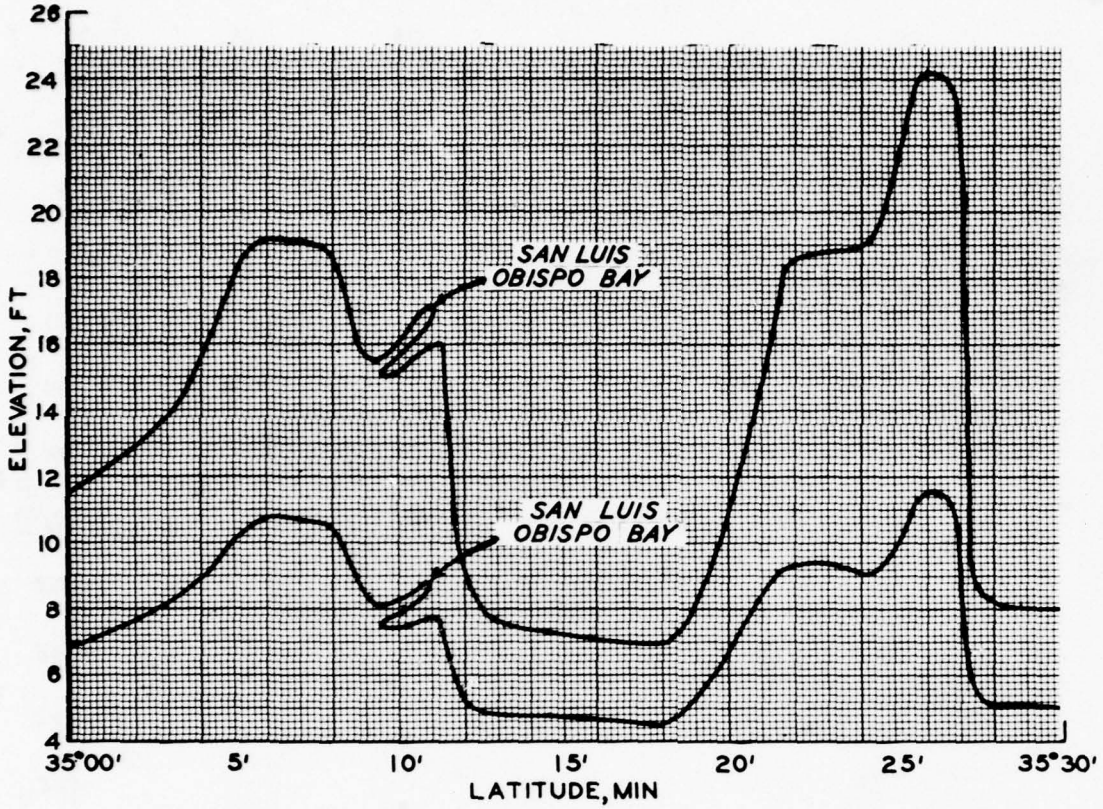

100- AND 500-YEAR ELEVATIONS VS LOCATION

LATITUDE 35°00' TO 35°30'

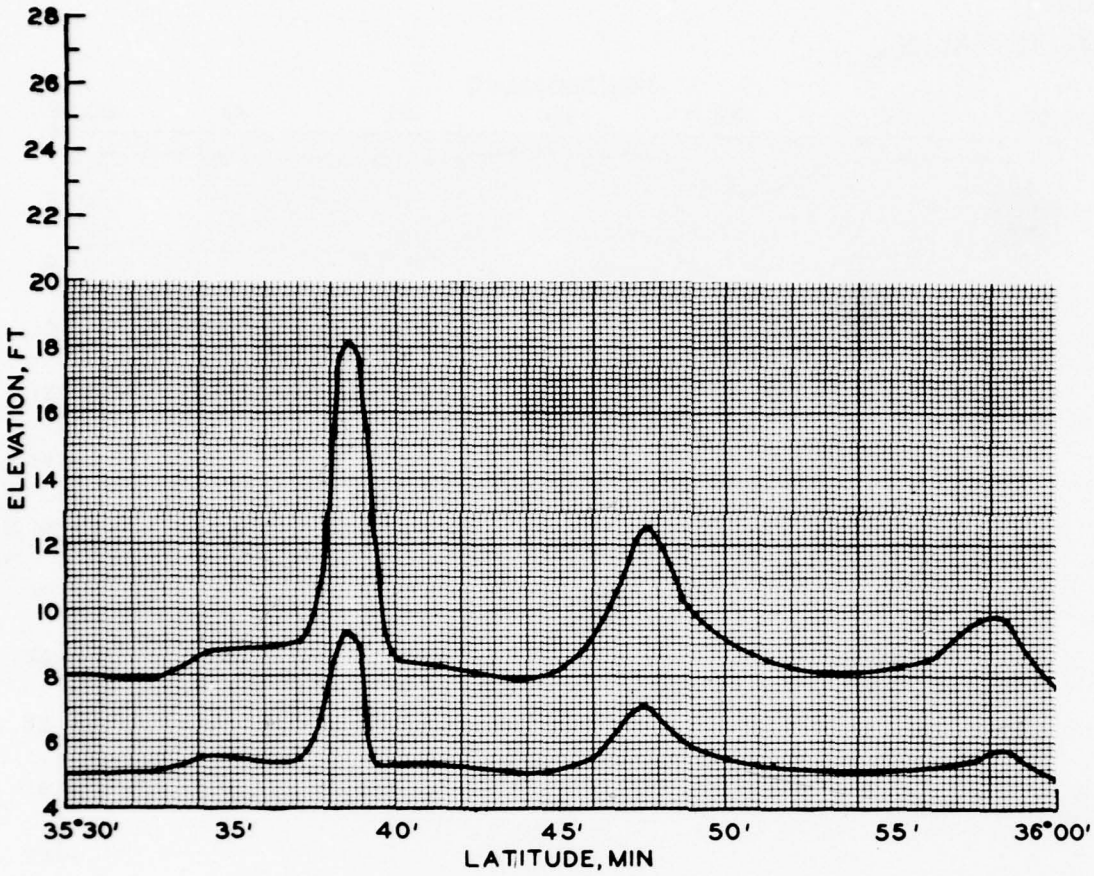

100- AND 500-YEAR ELEVATIONS VS LOCATION

LATITUDE 35°30' TO 36°00'

PLATE 5

PLATE 6

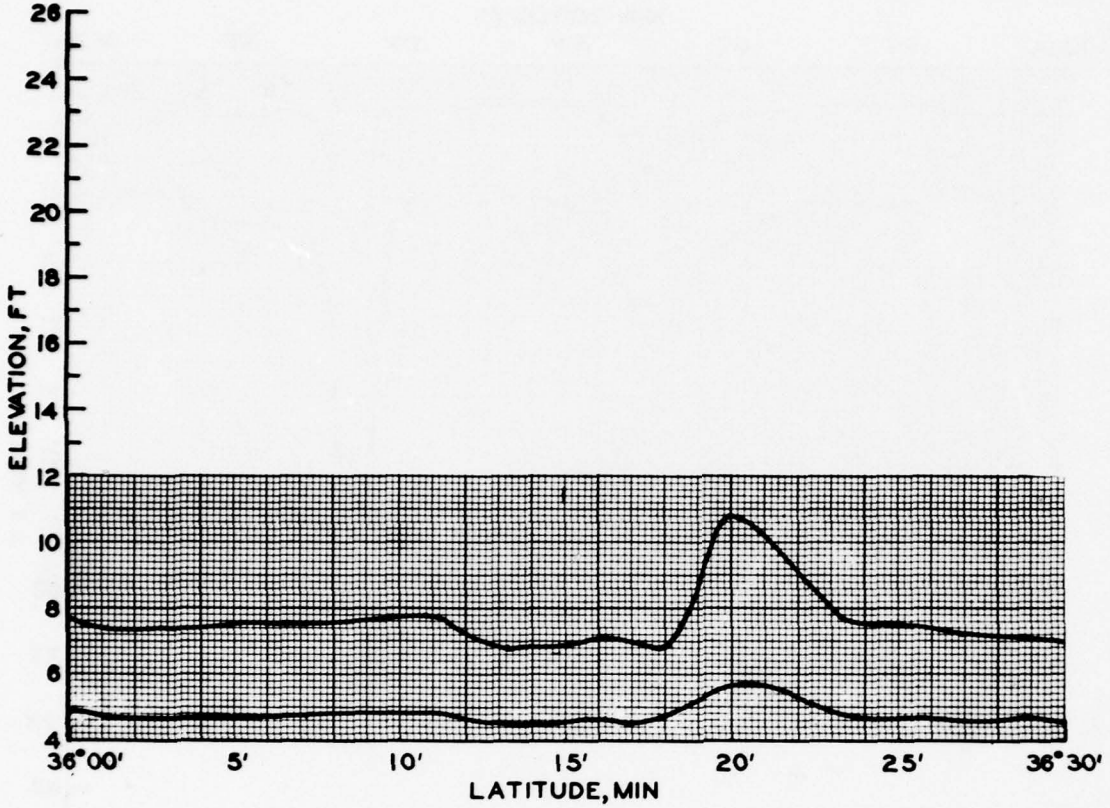

100- AND 500-YEAR ELEVATIONS VS LOCATION

LATITUDE 36°00′ TO 36°30′

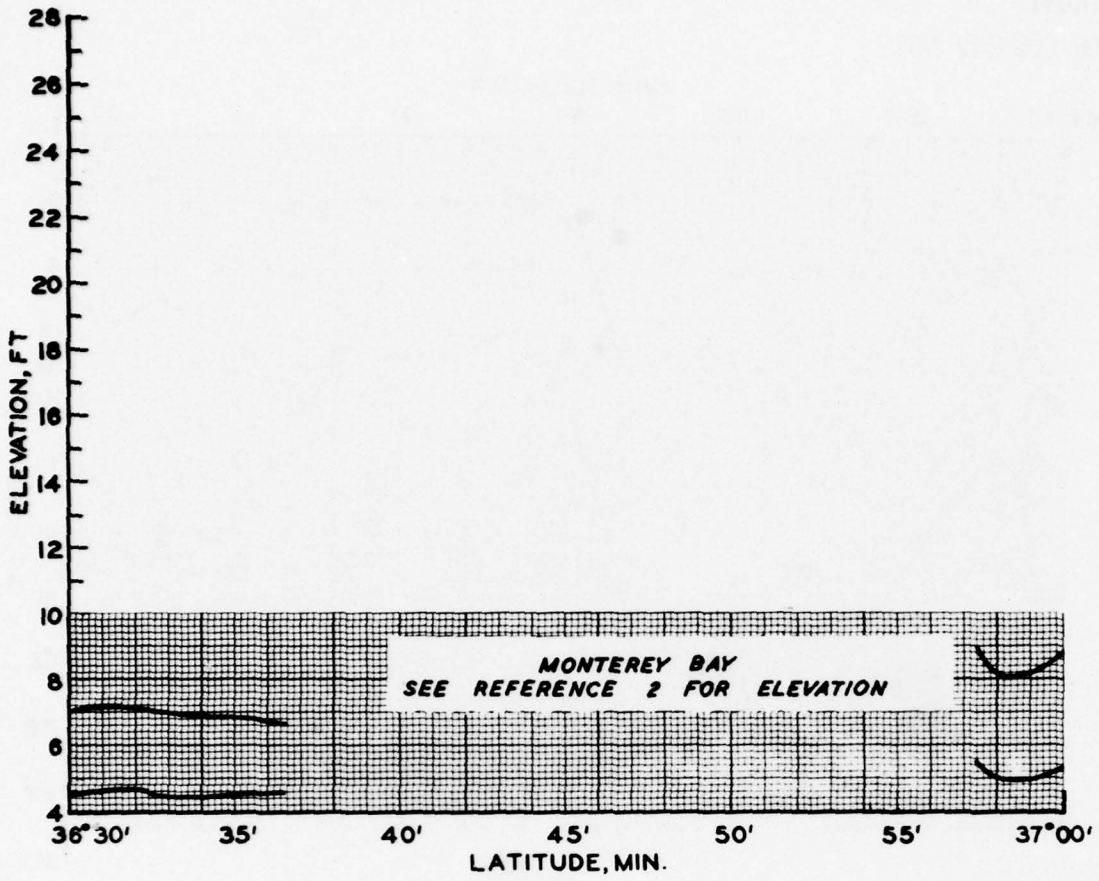

100- AND 500-YEAR ELEVATIONS VS LOCATION

LATITUDE 36°30' TO 37°00'

PLATE 7

PLATE 8

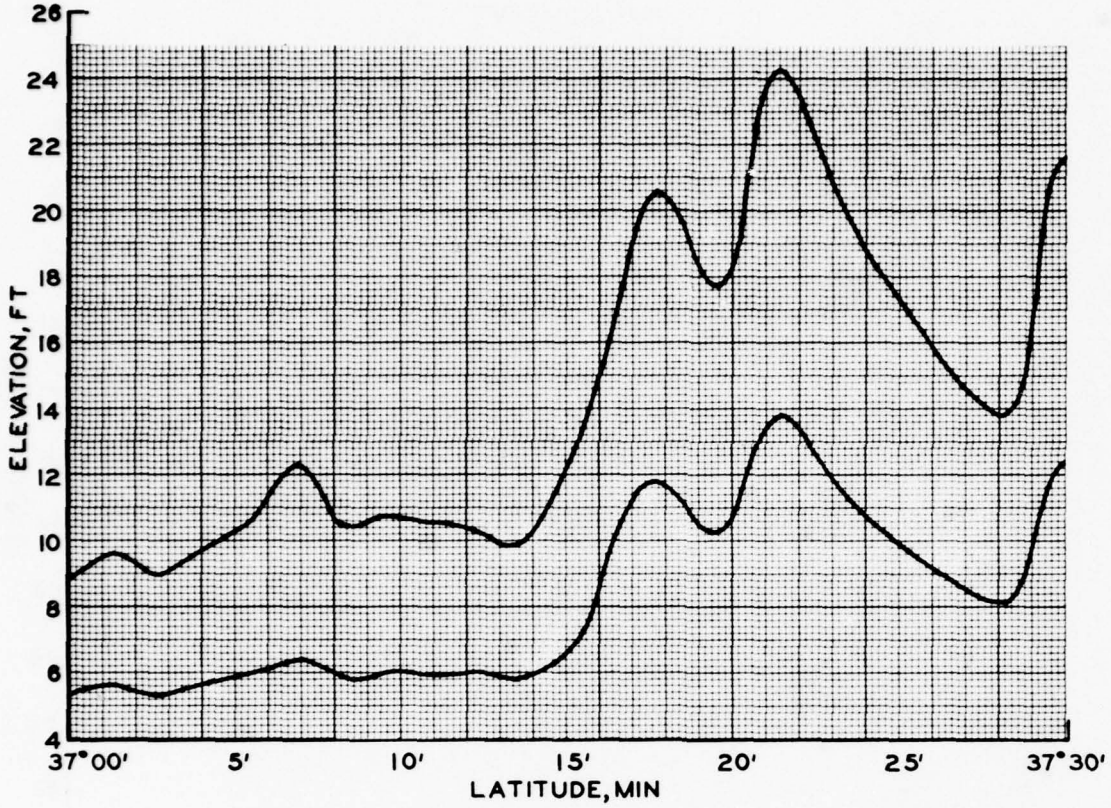

100- AND 500-YEAR ELEVATIONS VS LOCATION

LATITUDE 37°00' TO 37°30'

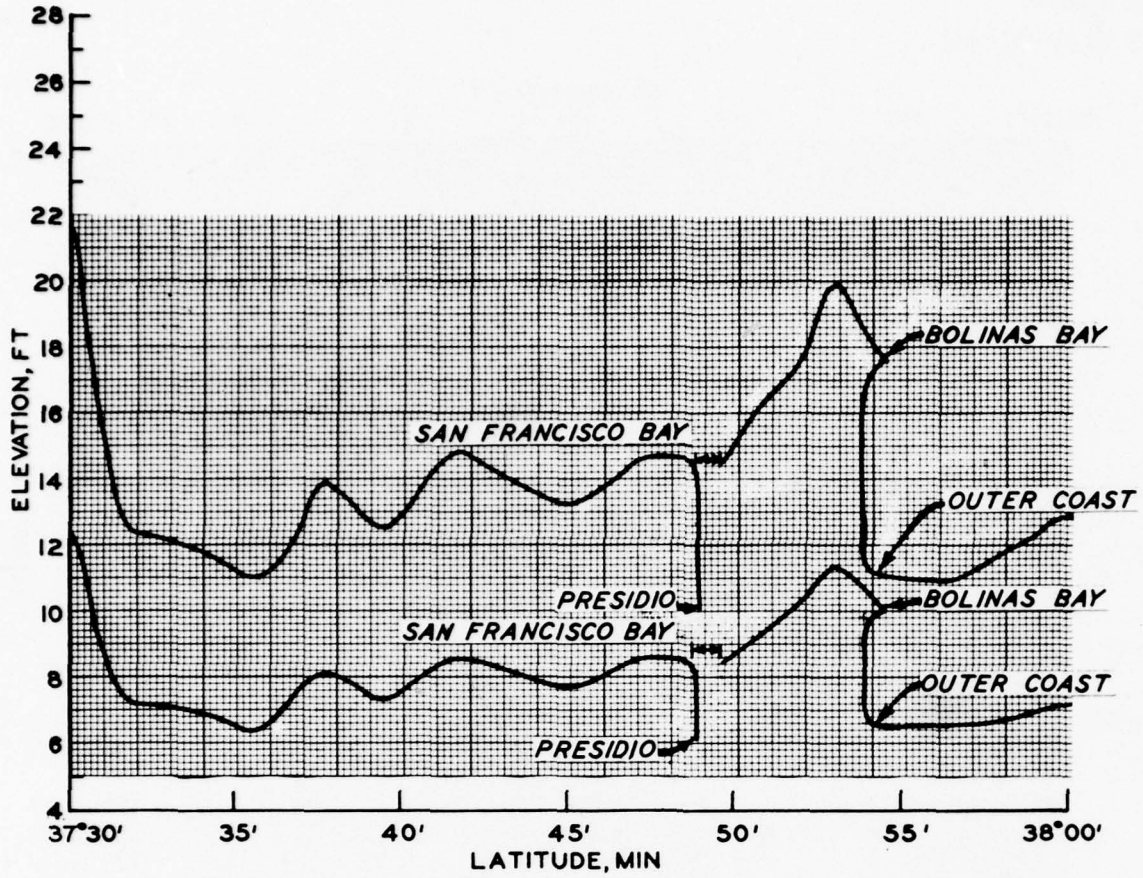

100- AND 500-YEAR ELEVATIONS VS LOCATION

LATITUDE 37°30' TO 38°00'

PLATE 9

PLATE 10

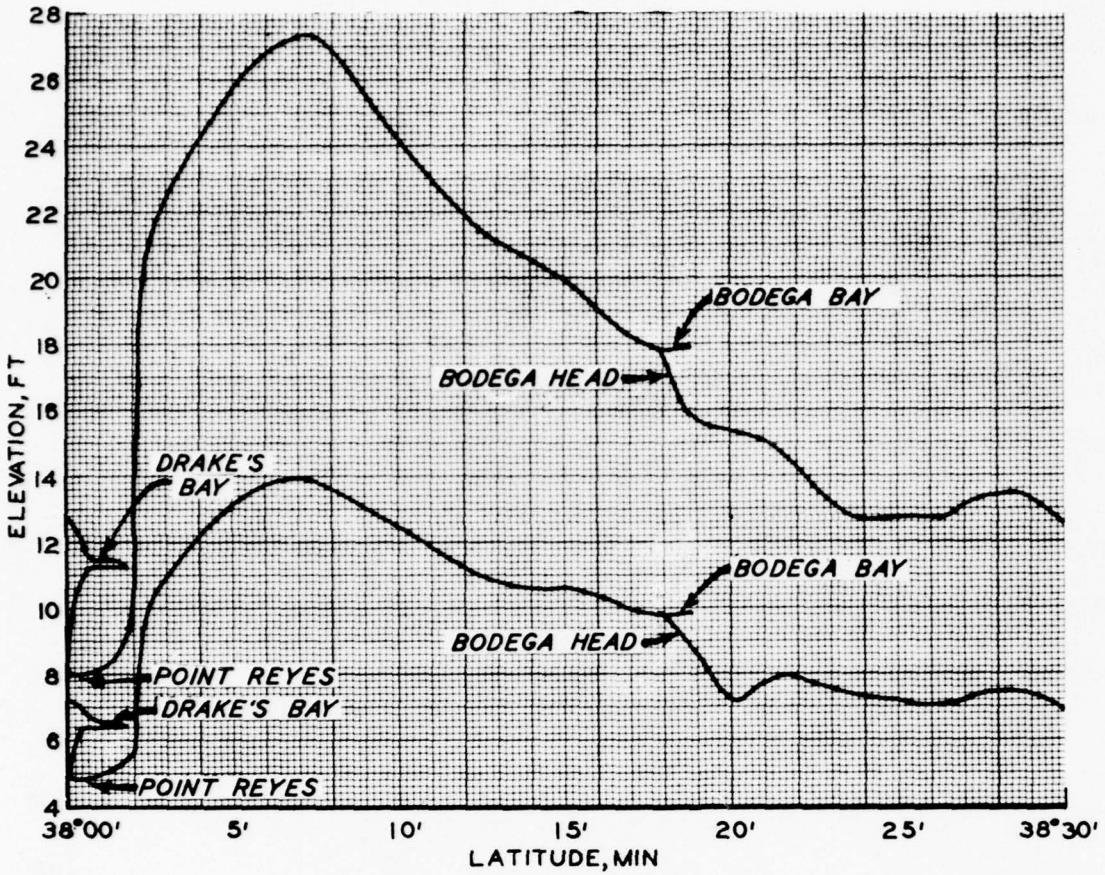

100- AND 500-YEAR ELEVATIONS VS LOCATION

LATITUDE 38°00' TO 38°30'

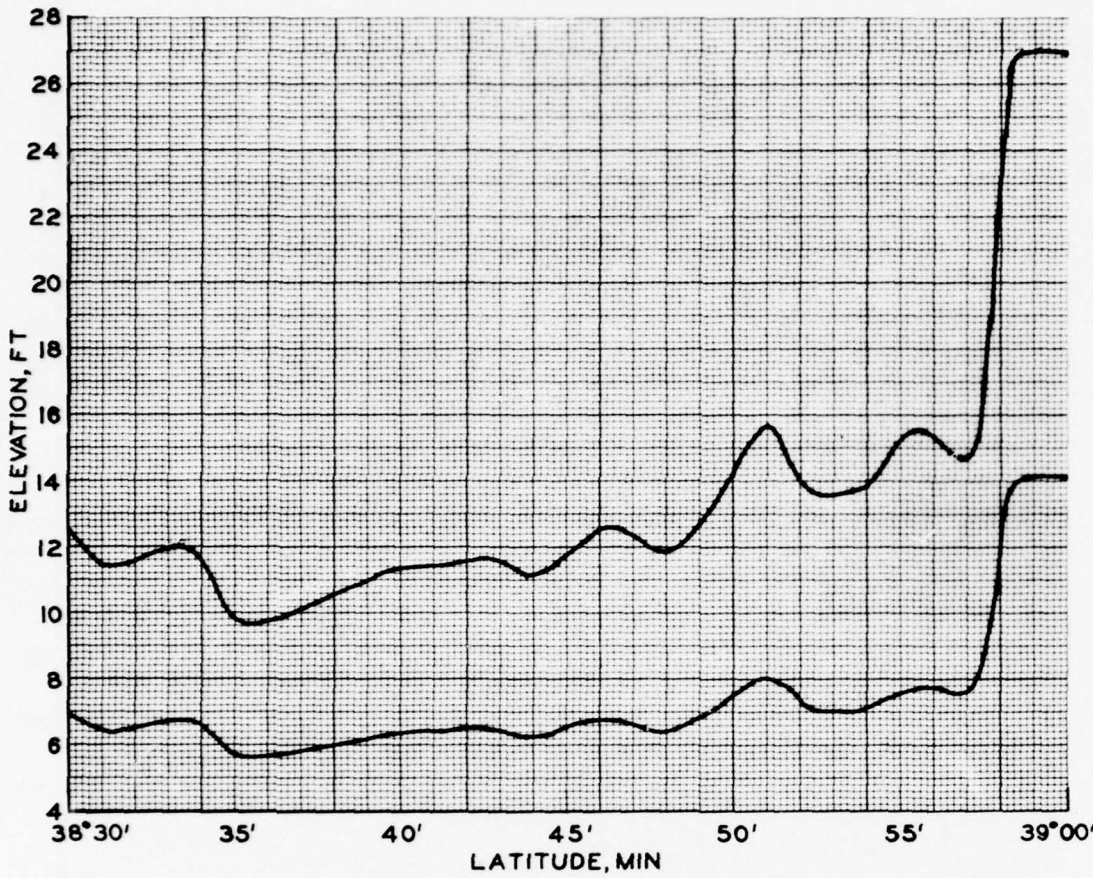

100- AND 500-YEAR ELEVATIONS VS LOCATION

LATITUDE 38°30′ TO 39°00′

PLATE 11

PLATE 12

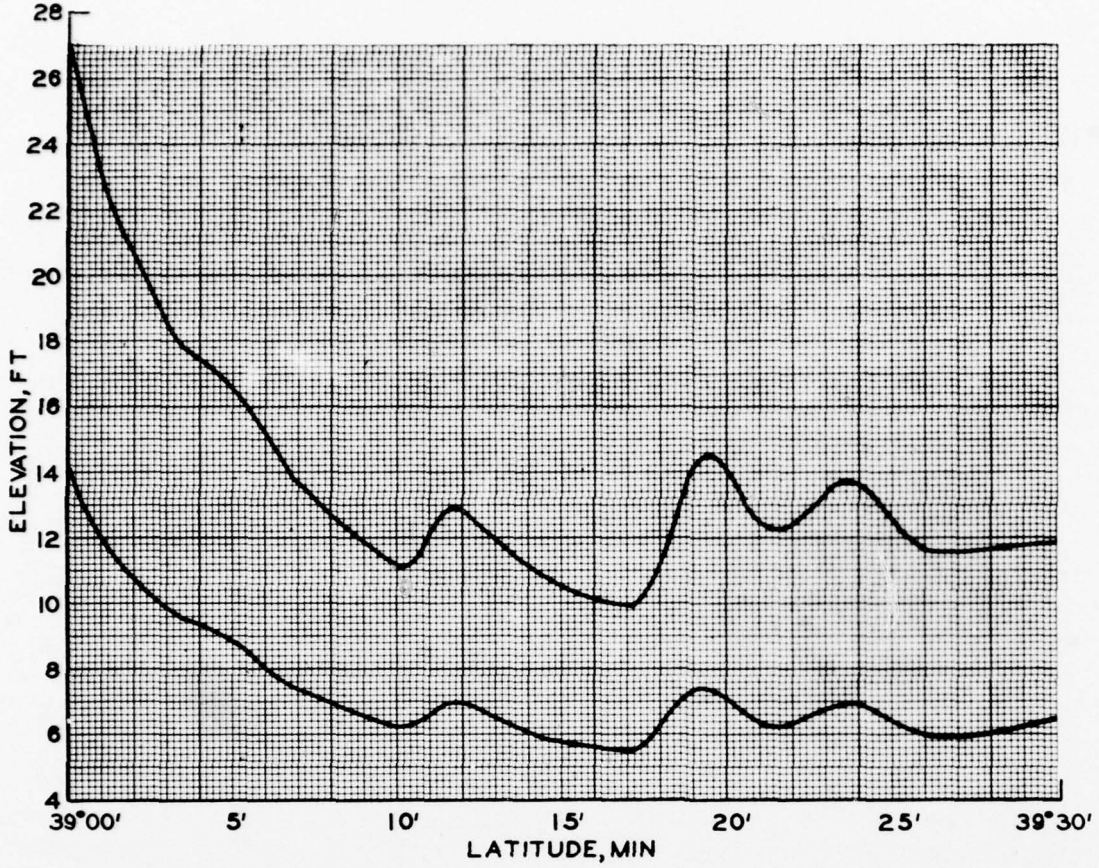

100- AND 500-YEAR ELEVATIONS VS LOCATION

LATITUDE 39°00' TO 39°30'

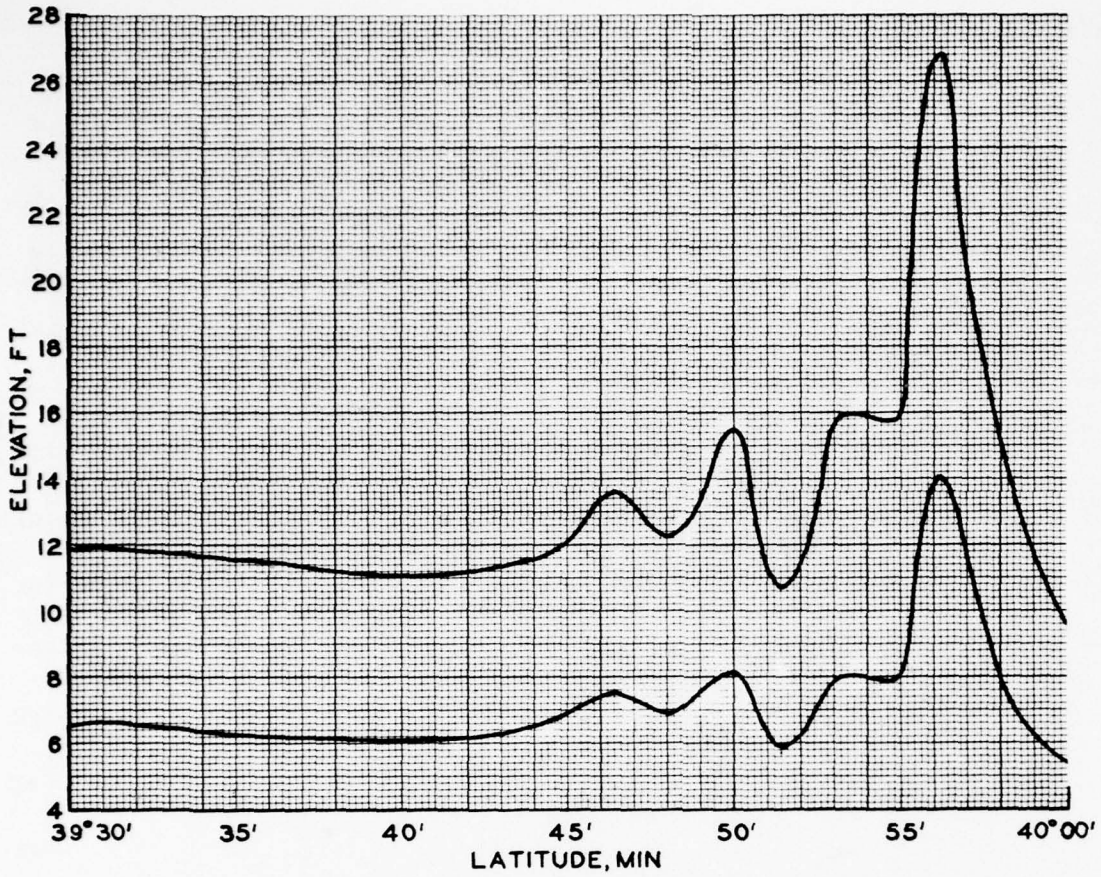

100- AND 500-YEAR ELEVATIONS VS LOCATION

LATITUDE 39°30' TO 40°00'

PLATE 13

PLATE 14

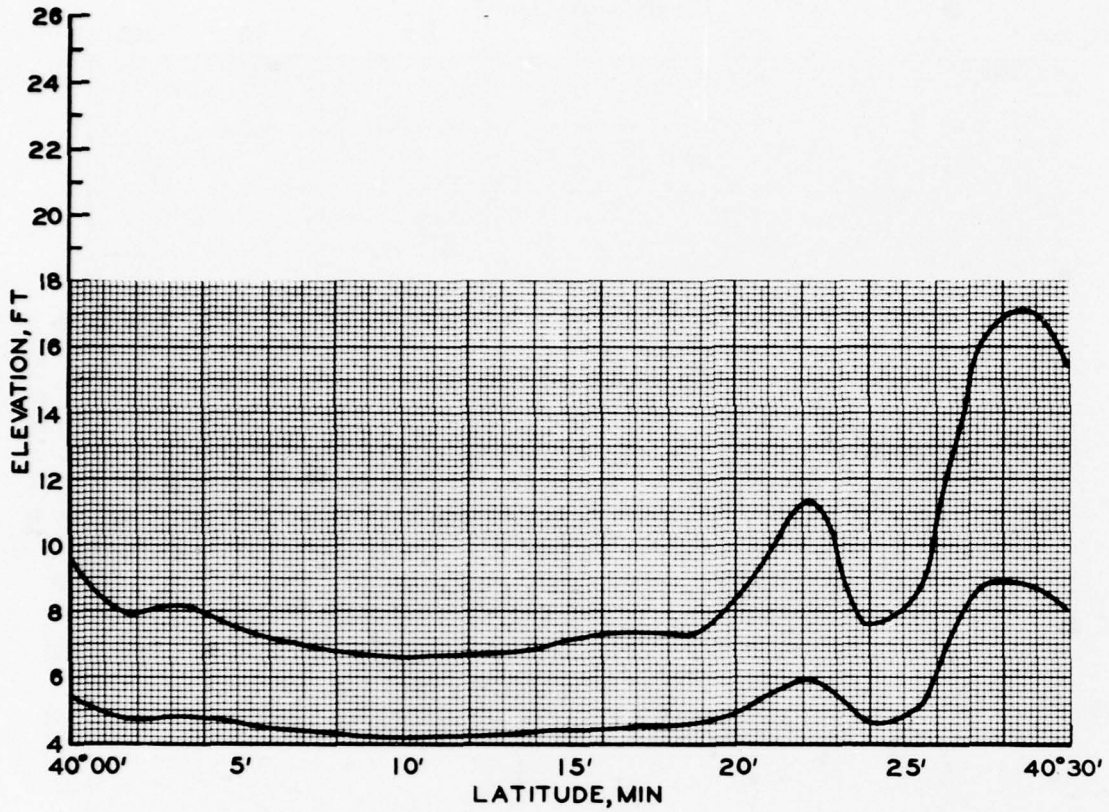

100- AND 500-YEAR ELEVATIONS VS LOCATION

LATITUDE 40°00′ TO 40°30′

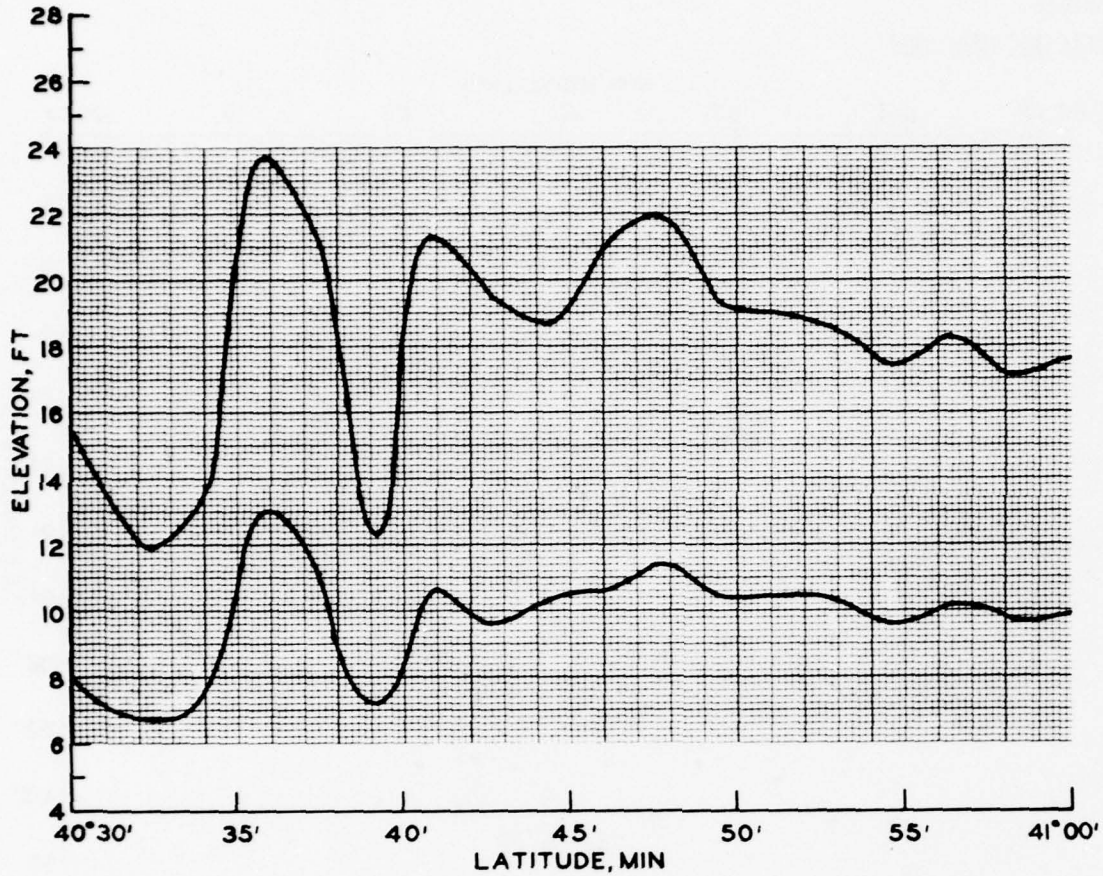

100- AND 500-YEAR ELEVATIONS VS LOCATION

LATITUDE 40°30' TO 41°00'

PLATE 15

PLATE 16

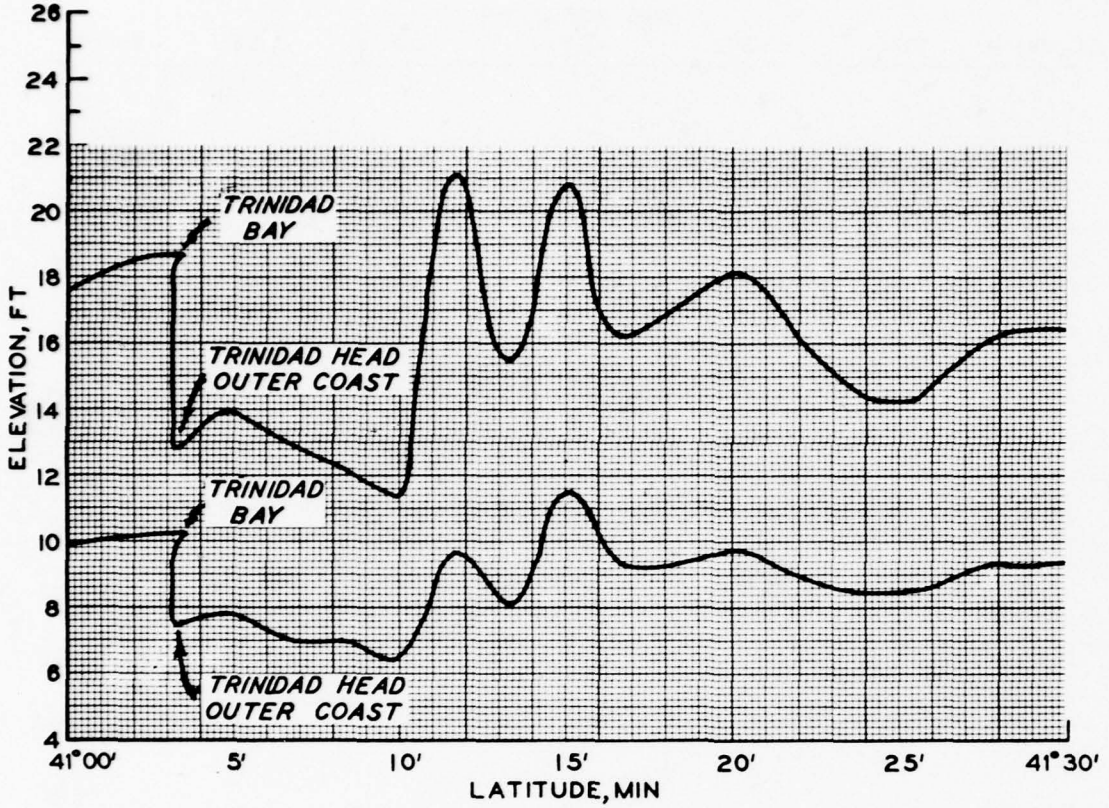

100- AND 500-YEAR ELEVATIONS VS LOCATION

LATITUDE 41°00′ TO 41°30′

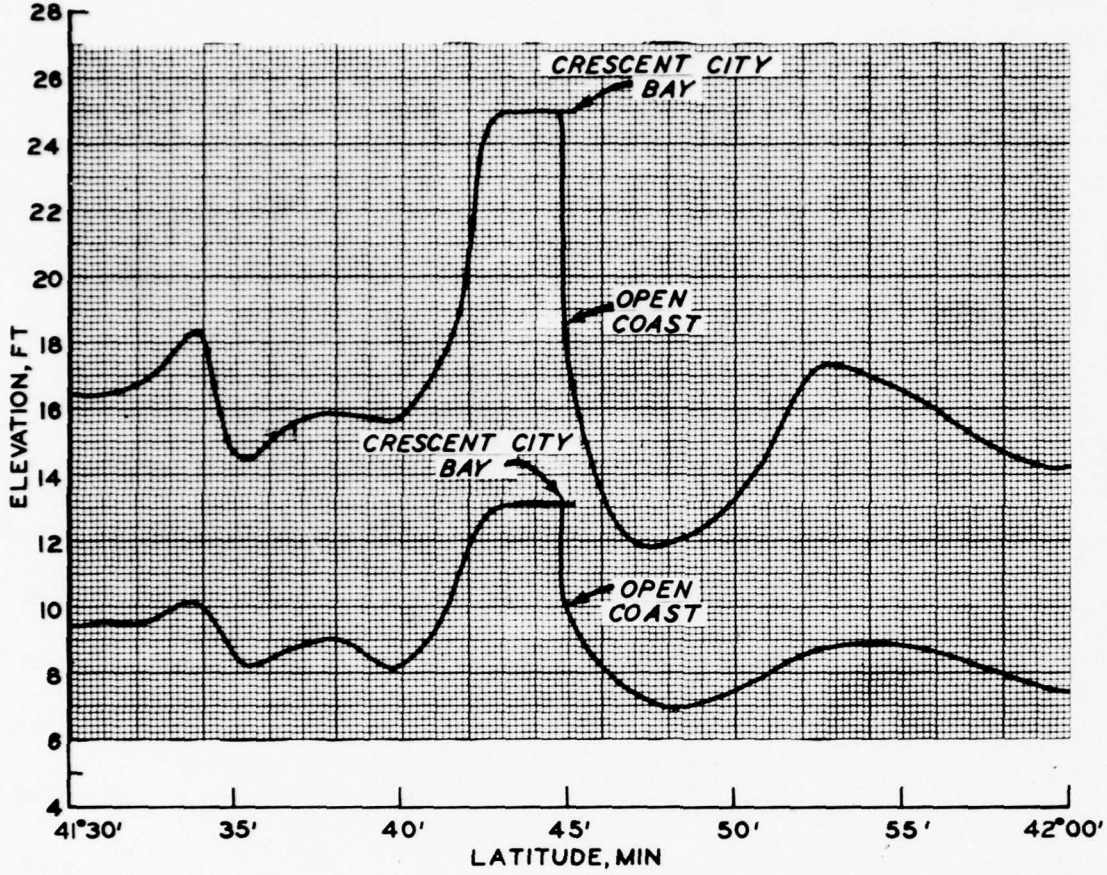

100- AND 500-YEAR ELEVATIONS VS LOCATION

LATITUDE 41°30' TO 42°00'

PLATE 17

PLATE 18

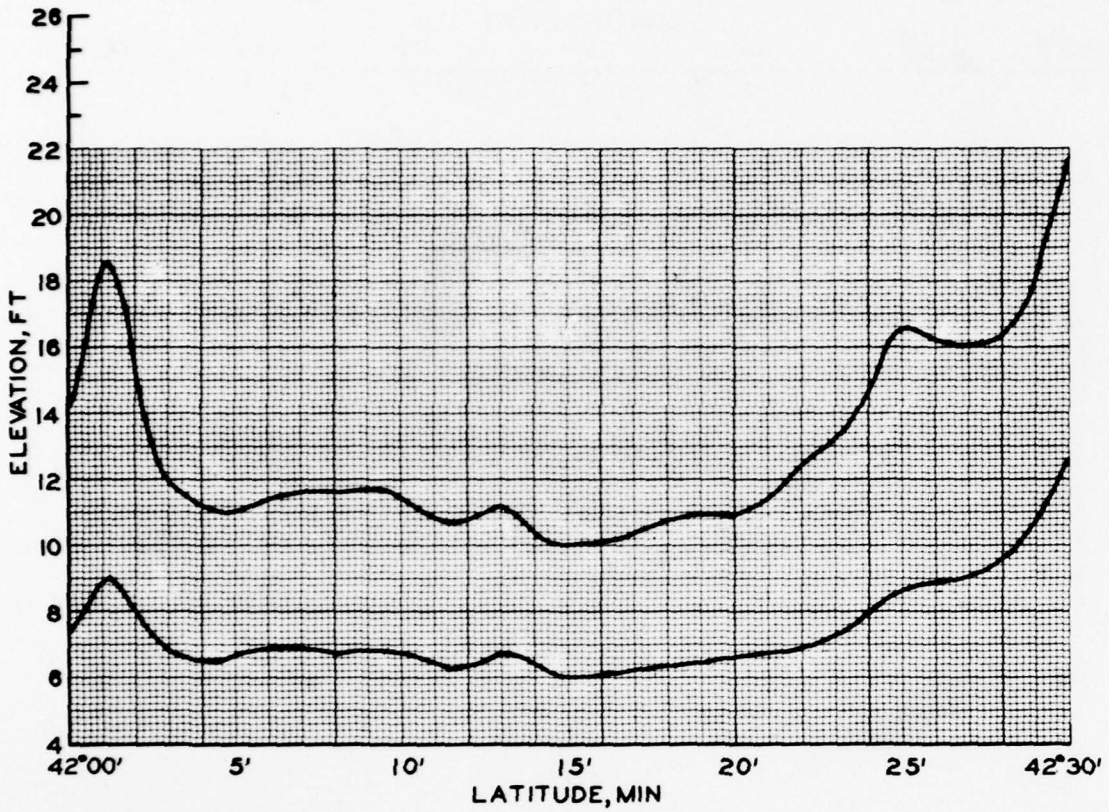

100- AND 500-YEAR ELEVATIONS VS LOCATION

LATITUDE 42°00' TO 42°30'

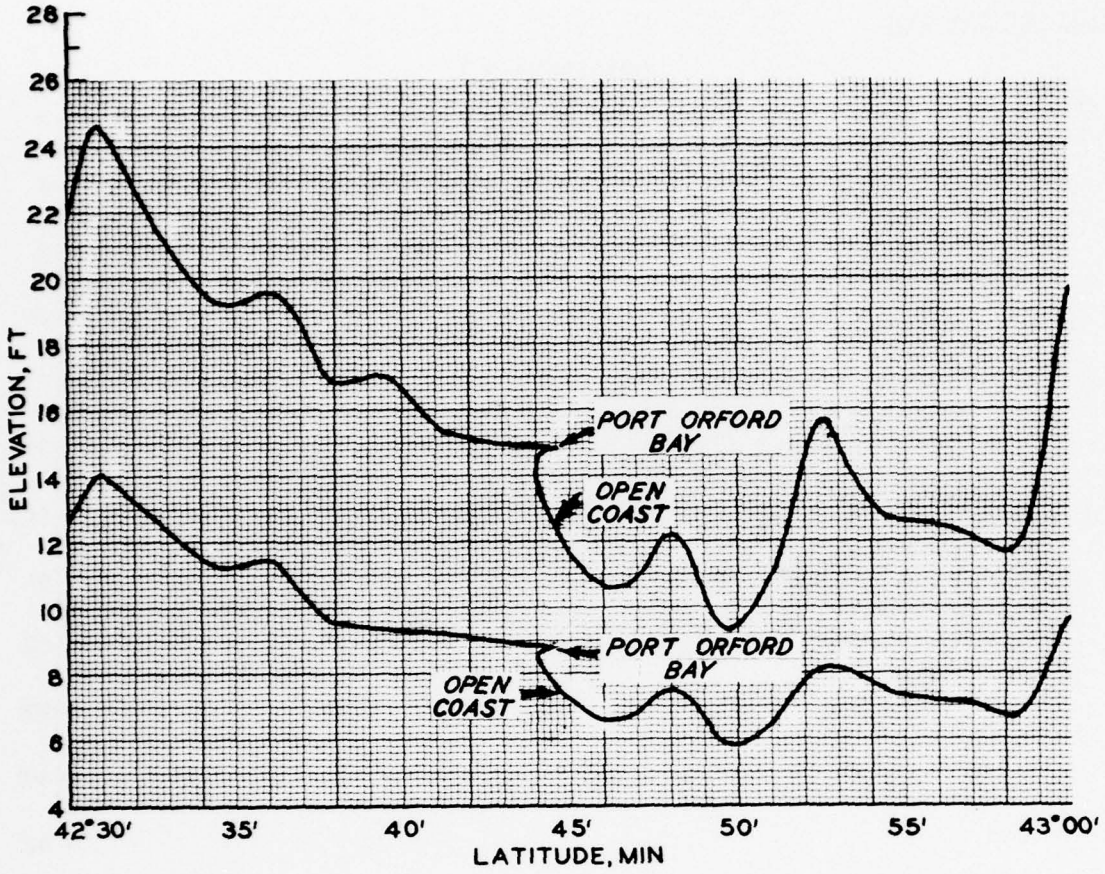

100- AND 500-YEAR ELEVATIONS VS LOCATION

LATITUDE 42°30′ TO 43°00′

PLATE 19

PLATE 20

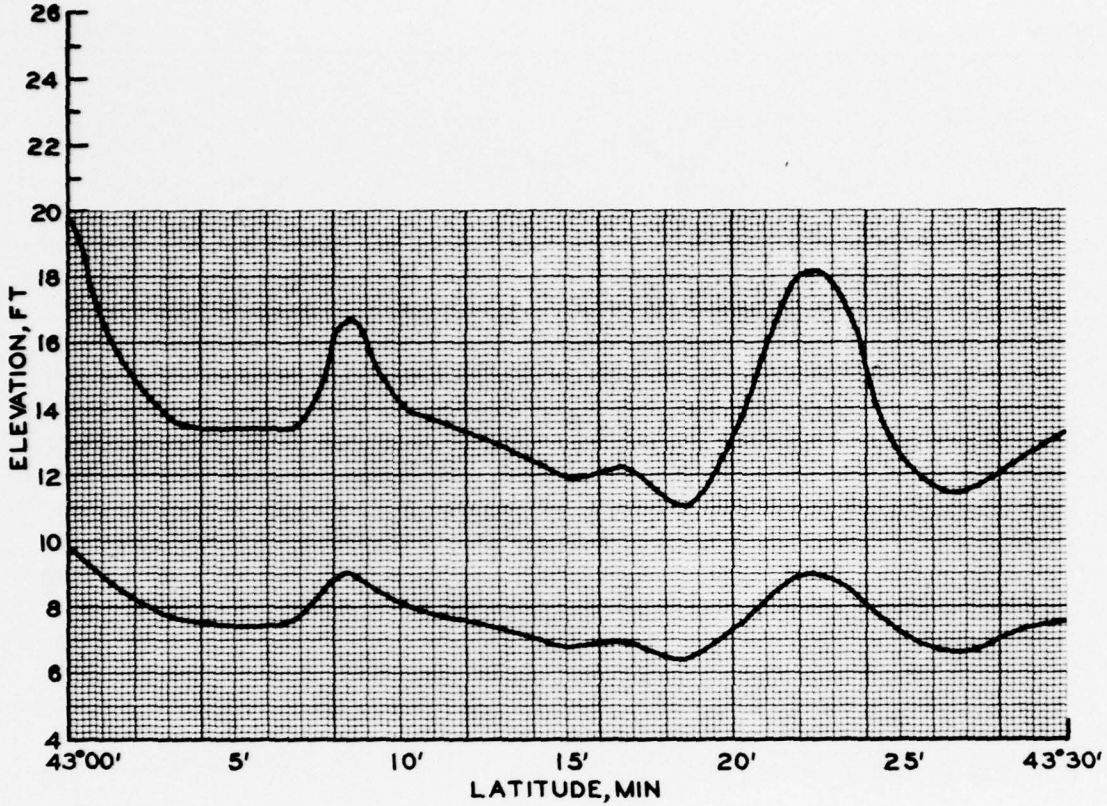

100- AND 500-YEAR ELEVATIONS VS LOCATION

LATITUDE 43°00' TO 43°30'

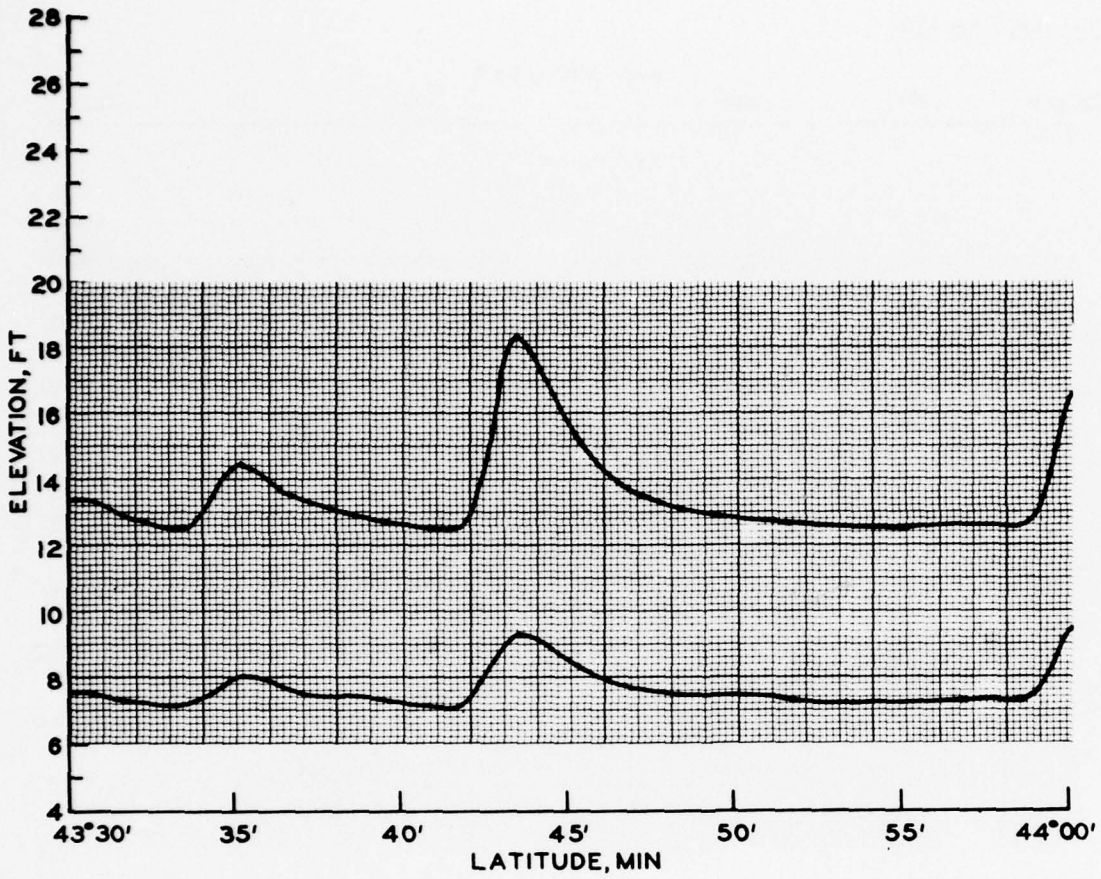

100- AND 500-YEAR ELEVATIONS VS LOCATION

LATITUDE 43°30' TO 44°00'

PLATE 21

PLATE 22

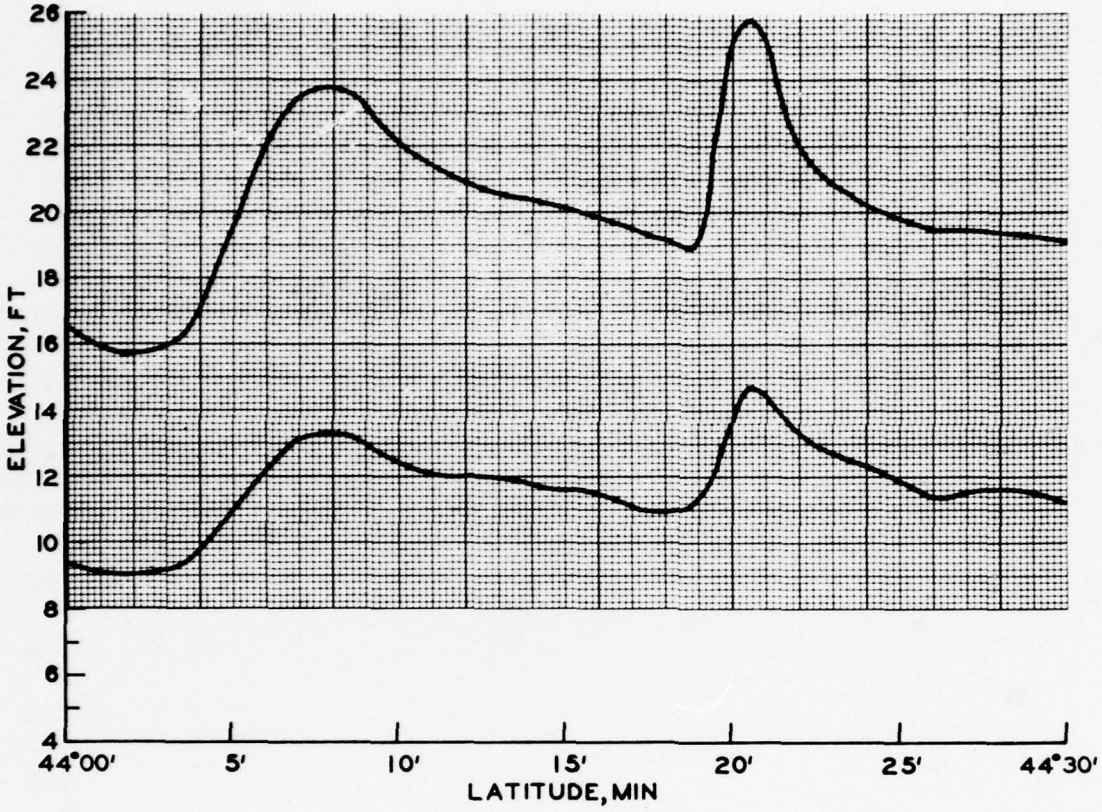

100- AND 500-YEAR ELEVATIONS VS LOCATION

LATITUDE 44°00' TO 44°30'

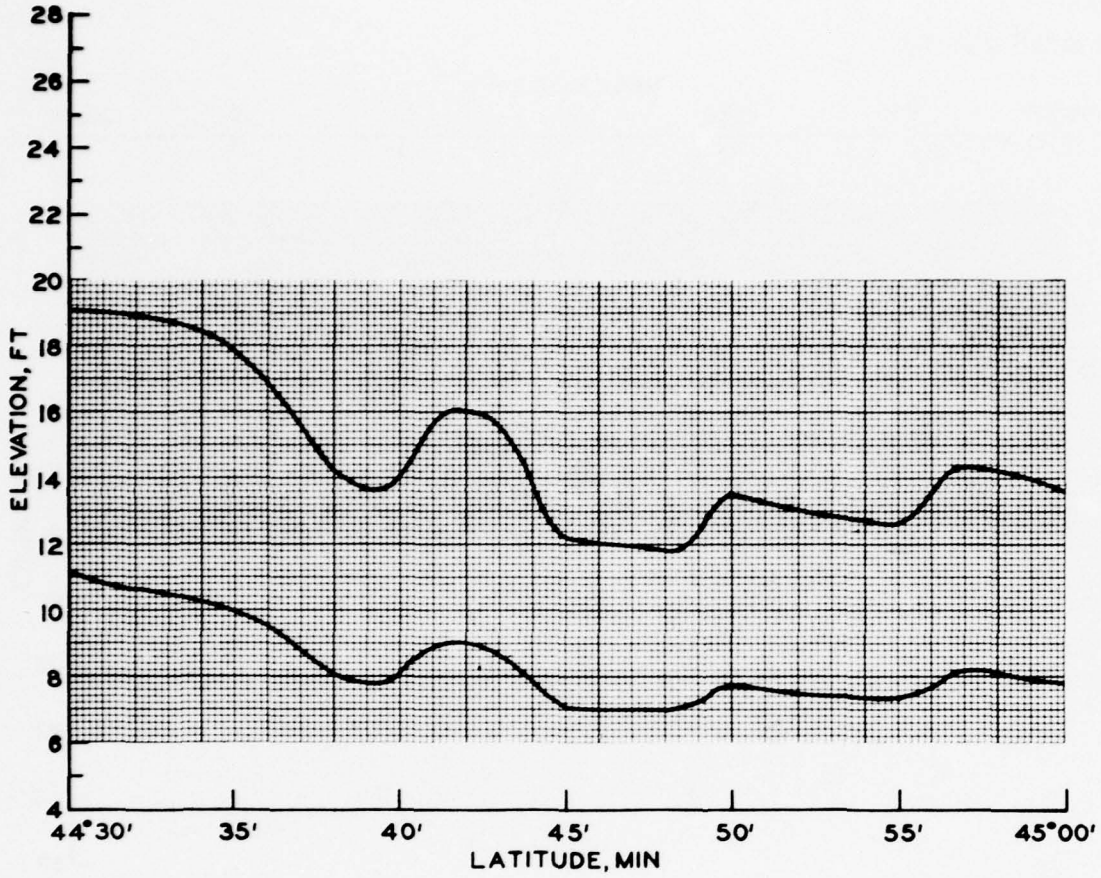

100- AND 500-YEAR ELEVATIONS VS LOCATION

LATITUDE 44°30′ TO 45°00′

PLATE 23

PLATE 24

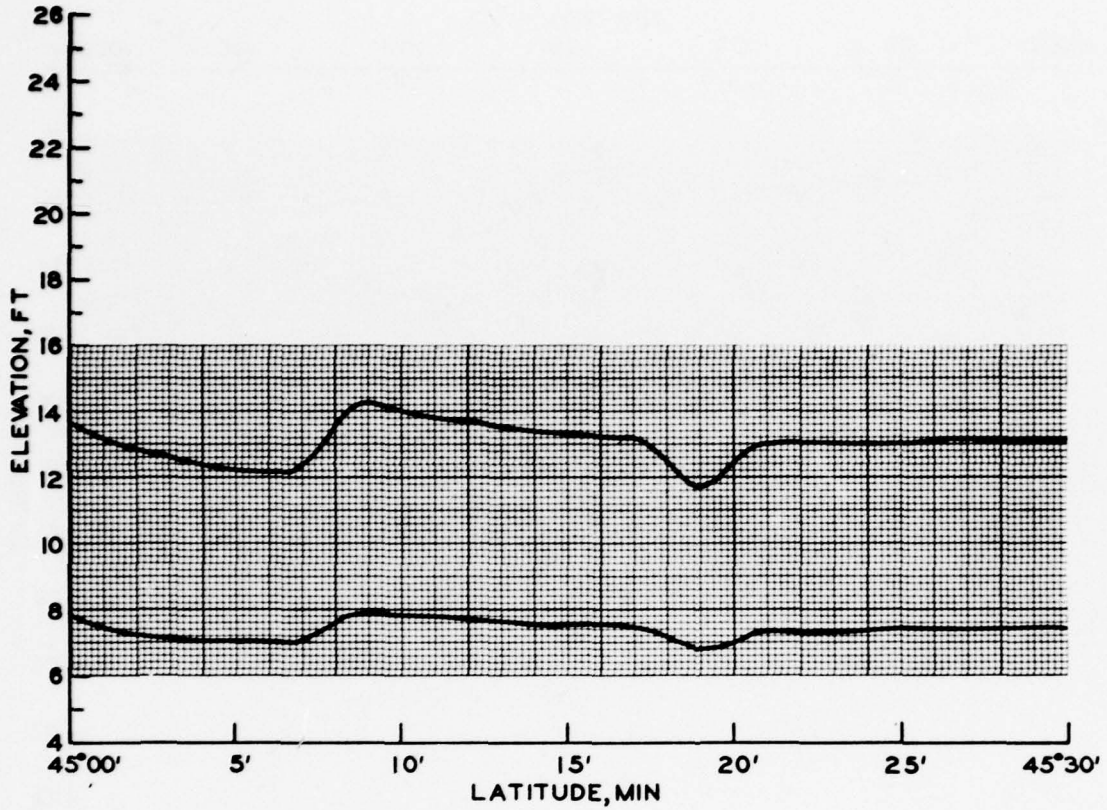

100- AND 500-YEAR ELEVATIONS VS LOCATION

LATITUDE 45°00' TO 45°30'

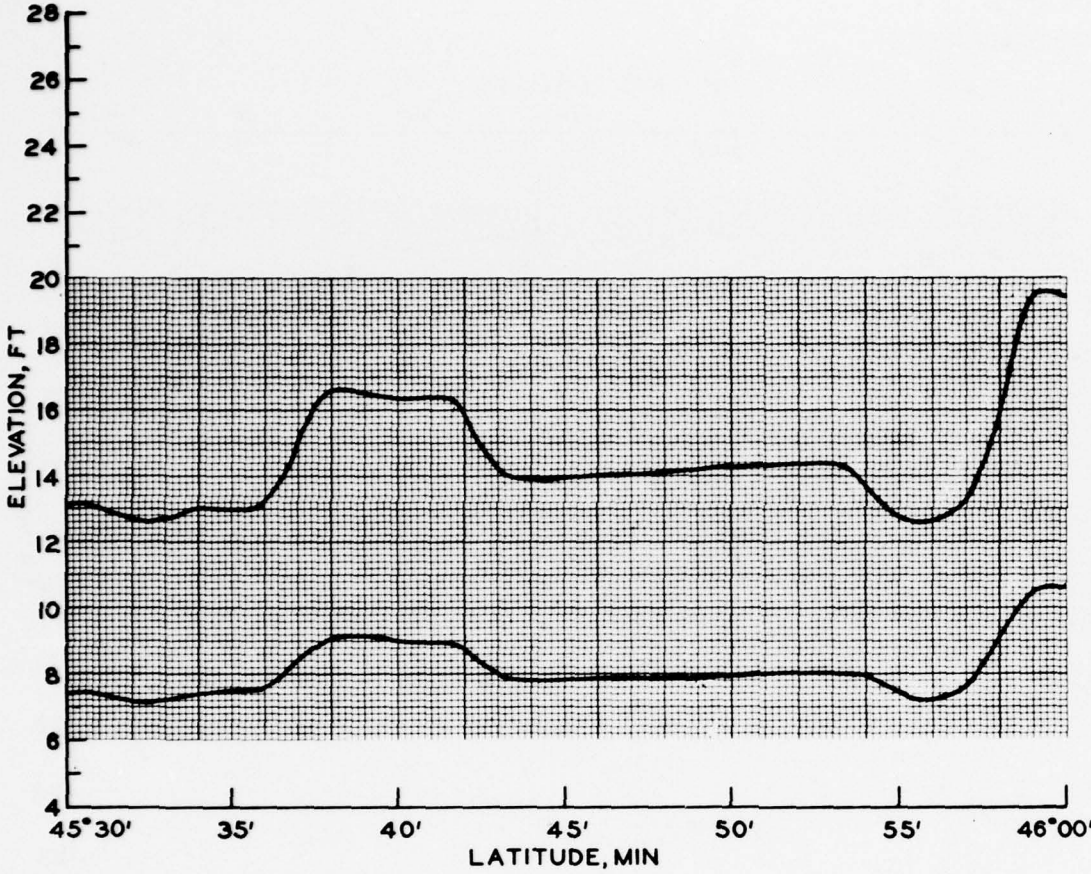

100- AND 500-YEAR ELEVATIONS VS LOCATION

LATITUDE 45°30′ TO 46°00′

PLATE 25

PLATE 26

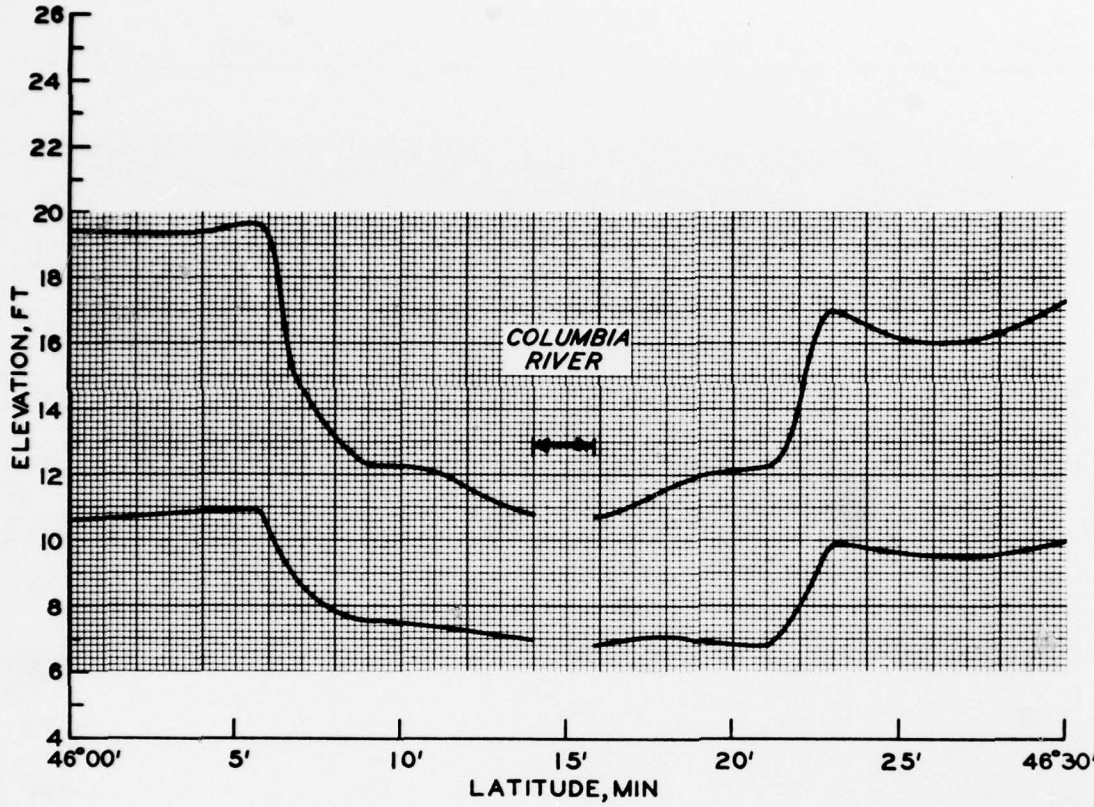

100- AND 500-YEAR ELEVATIONS VS LOCATION

LATITUDE 46°00′ TO 46°30′

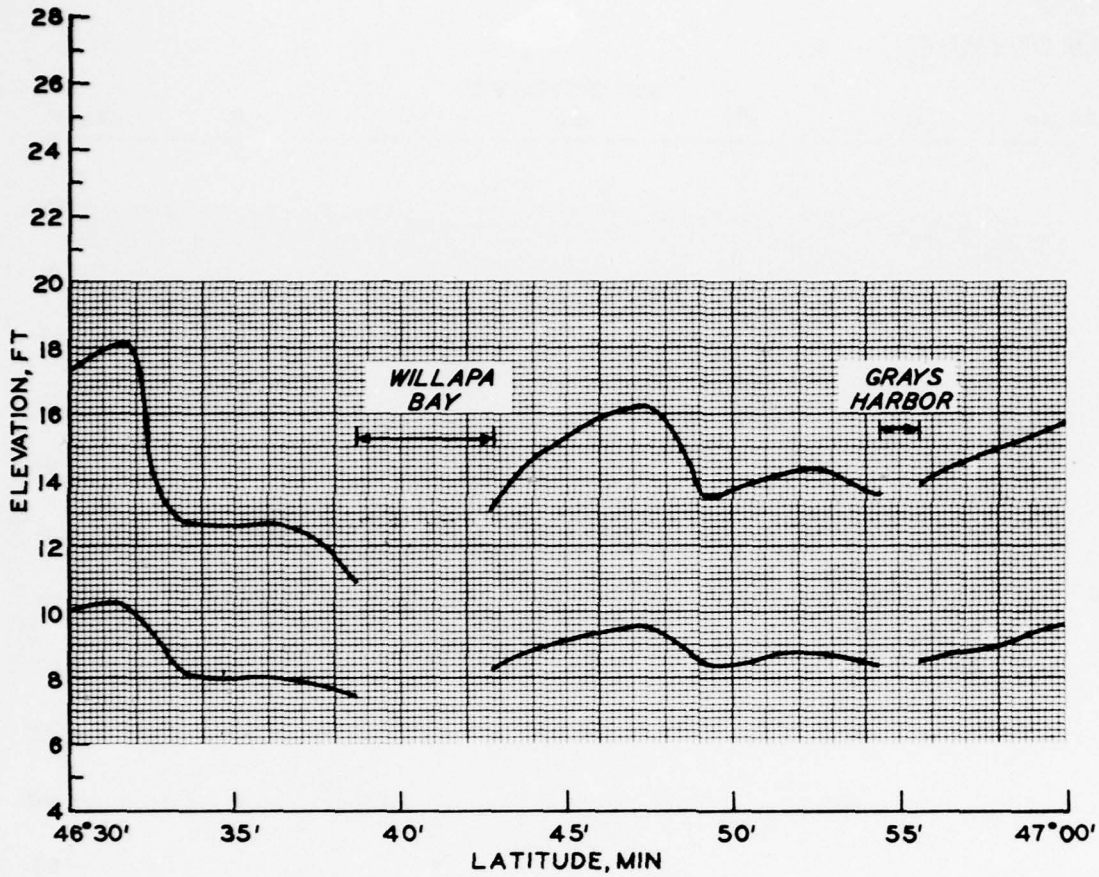

100- AND 500-YEAR ELEVATIONS VS LOCATION

LATITUDE 46°30' TO 47°00'

PLATE 27

PLATE 28

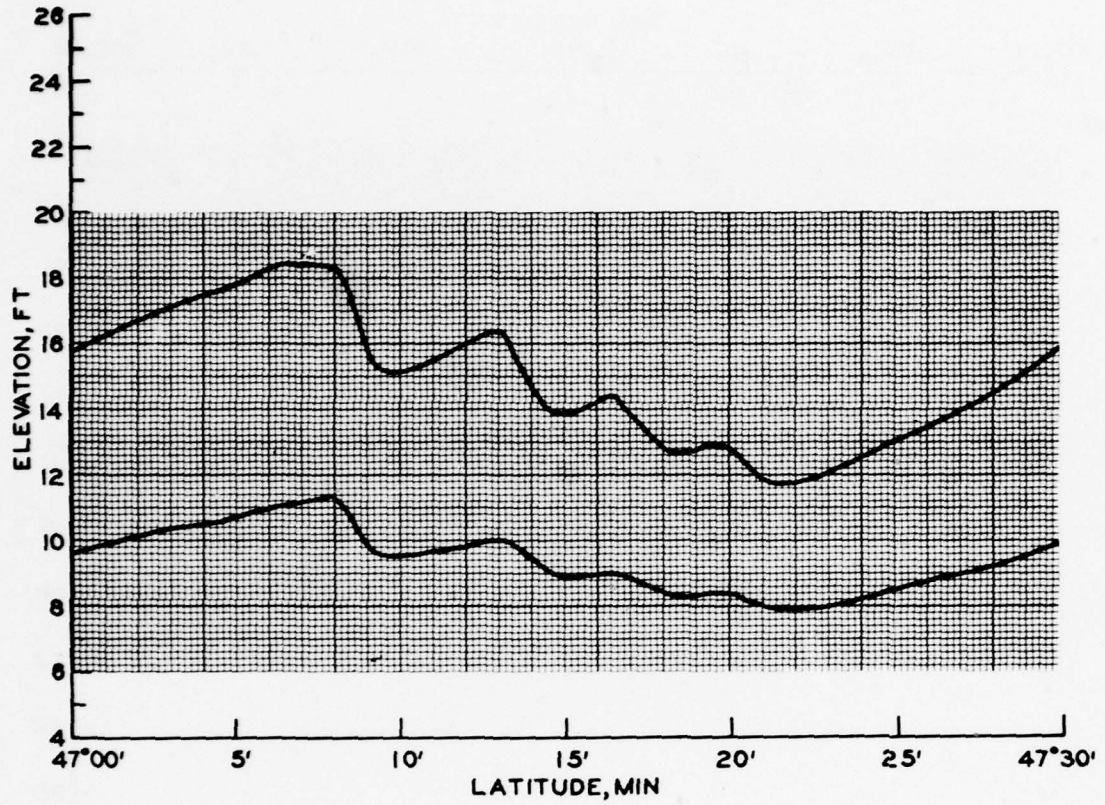

100- AND 500-YEAR ELEVATIONS VS LOCATION

LATITUDE 47°00′ TO 47°30′

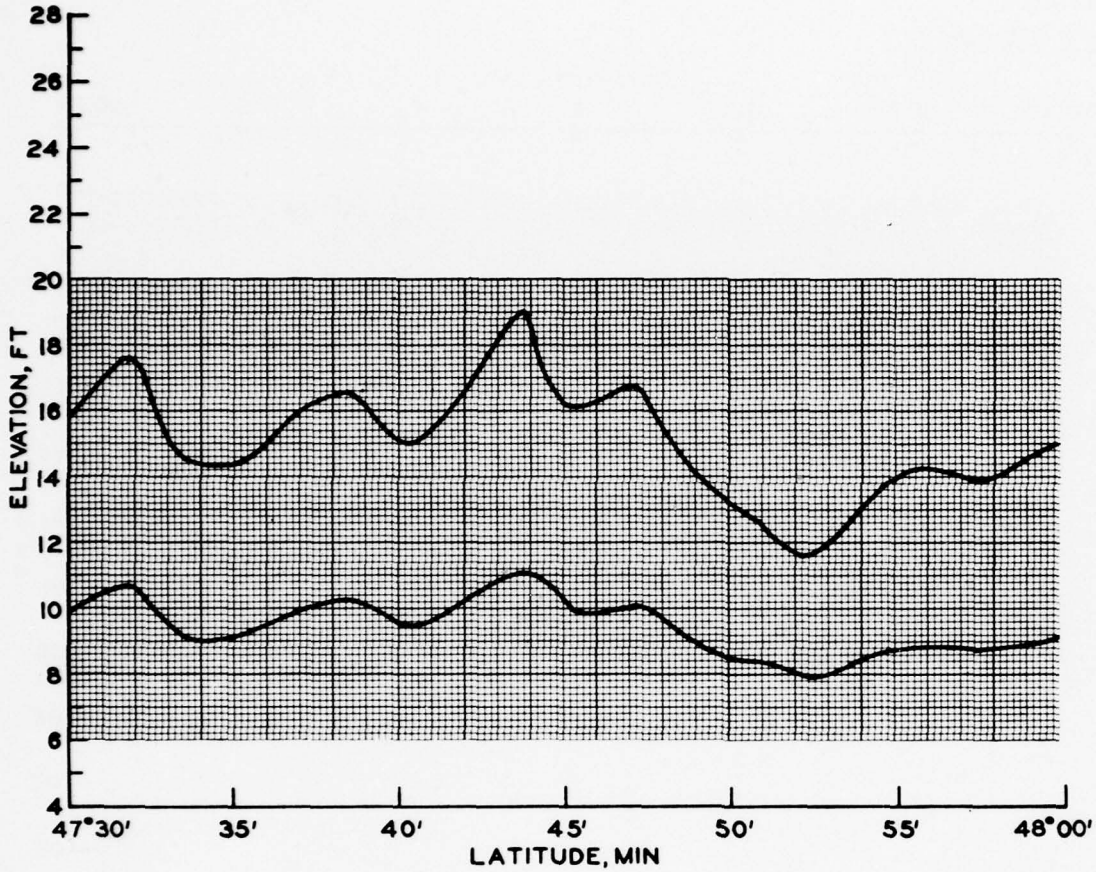

100- AND 500-YEAR ELEVATIONS VS LOCATION

LATITUDE 47°30' TO 48°00'

PLATE 29

PLATE 30

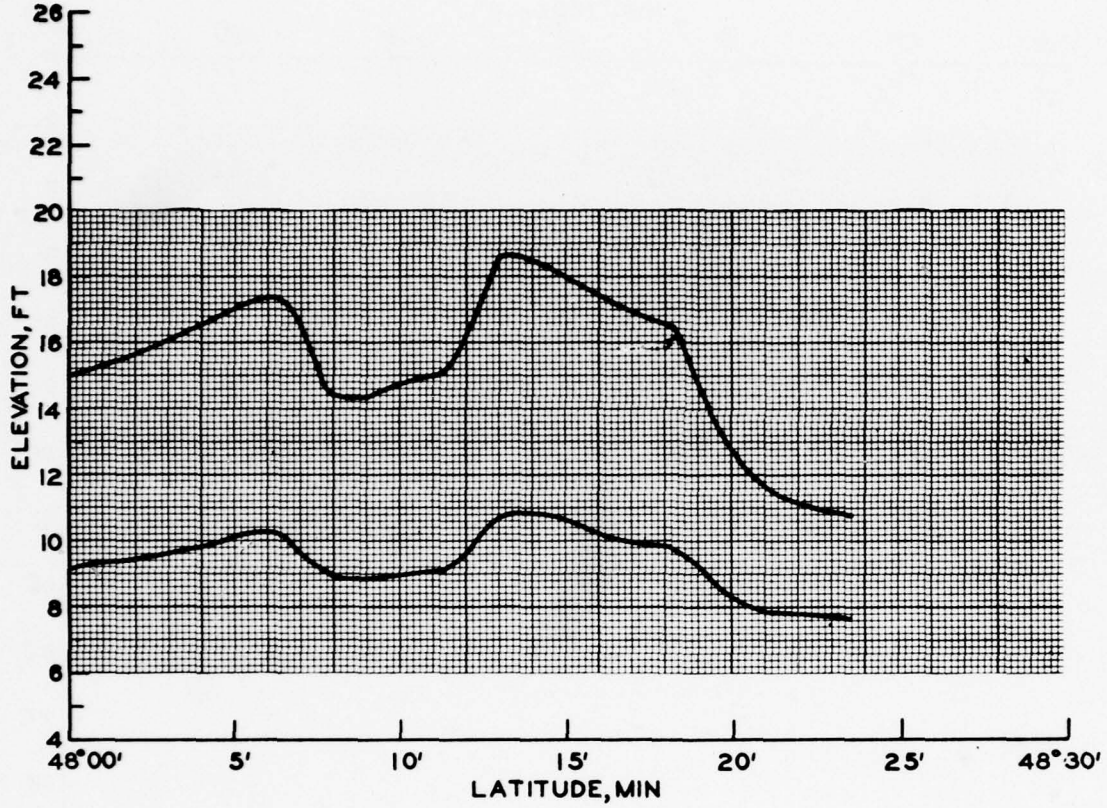

100- AND 500-YEAR ELEVATIONS VS LOCATION

LATITUDE 48°00' TO 48°23.6'

APPENDIX A: NOTATION

a	Length of major axis of elliptical source, miles
A	Probability constant
b	Length of minor axis of elliptical source, miles
C	Chezy coefficient, $ft^{1/2}/sec$
C_m	Amplitude of m^{th} tidal constituent, ft
e	
g	Acceleration due to gravity, ft/sec^2
h	Water depth, ft
H_a	Wave height in direction of major axis of ellipse, ft
H_b	Wave height in direction of minor axis of ellipse, ft
H_{avg}	Average runup over a coast, m
i	Tsunami intensity
$n( )$	Tsunami probability function
$P( )$	Cumulative probability distribution for runup
t	Time, sec
T_B^x	Bottom stress in x-direction, ft^2/sec^2
T_B^y	Bottom stress y-direction, ft^2/sec^2
U	Water velocity in x-direction, ft/sec
V	Water velocity in y-direction, ft/sec
x	Spatial coordinate, ft
y	Spatial coordinate, ft
z	Water-surface elevation above mean sea level (msl), ft
α	Exponential constant, ft^{-1}
η	Wave height, ft
σ	Model variation
σ^2	Tidal variance, ft^2

In accordance with letter from DAEN-RDC, DAEN-ASI dated 22 July 1977, Subject: Facsimile Catalog Cards for Laboratory Technical Publications, a facsimile catalog card in Library of Congress MARC format is reproduced below.

Houston, James R
Type 16 flood insurance study: tsunami predictions for the west coast of the continental United States / by James R. Houston, Andrew W. Garcia. Vicksburg, Miss. : U. S. Waterways Experiment Station ; Springfield, Va. : available from National Technical Information Service, 1978.
38, [1] p., 30 leaves of plates : ill. ; 27 cm. (Technical report - U. S. Army Engineer Waterways Experiment Station ; H-78-26)
Prepared for Federal Insurance Administration, Department of Housing and Urban Development, Washington, D. C.
References: p. 36-38.

1. Flood insurance. 2. Tsunamis. 3. Water wave run-up. I. Garcia, Andrew W., joint author. II. United States. Federal Insurance Administration. III. Title. IV. Series: United States. Waterways Experiment Station, Vicksburg, Miss. Technical report ; H-78-26.
TA7.W34 no.H-78-26